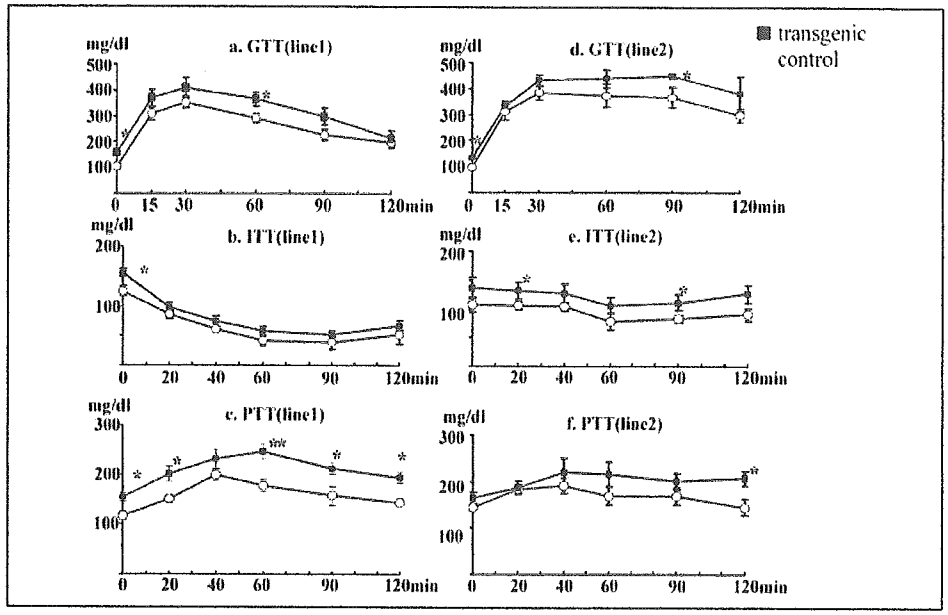

FIGURE 3. **Intraperitoneal glucose tolerance test (GTT), insulin tolerance test (ITT), and pyruvate tolerance test (PTT) in age-matched RELMβ transgenic (■, $n = 8$ for line 1 and $n = 7$ for line 2) and control mice (○, $n = 5$ for line 1 and $n = 7$ for line 2).** *a* and *d*, GTT for line 1 (age 16 weeks, fed a high fat diet for 4 weeks) and 2 (age 20 weeks, fed a high fat diet for 4 weeks) in comparison with the control mice fed a high fat diet for 4 weeks, respectively. *b* and *e*, ITT for line 1 (age 17 weeks, fed a high fat diet for 5 weeks) and 2 (age 21 weeks, fed a high fat diet for 5 weeks) in comparison with the control mice fed a high fat diet for 4 weeks, respectively. *c* and *f*, PTT for line 1 (age 18 weeks, fed a high fat diet for 6 weeks and 2 (age 22 weeks, fed a high fat diet for 6 weeks) in comparison with the control mice fed a high fat diet for 6 weeks, respectively. Values are presented as means ± S.E. Statistical significance is indicated by an *asterisk*: *, $p < 0.05$ for RELMβ transgenic mice *versus* control age-matched mice.

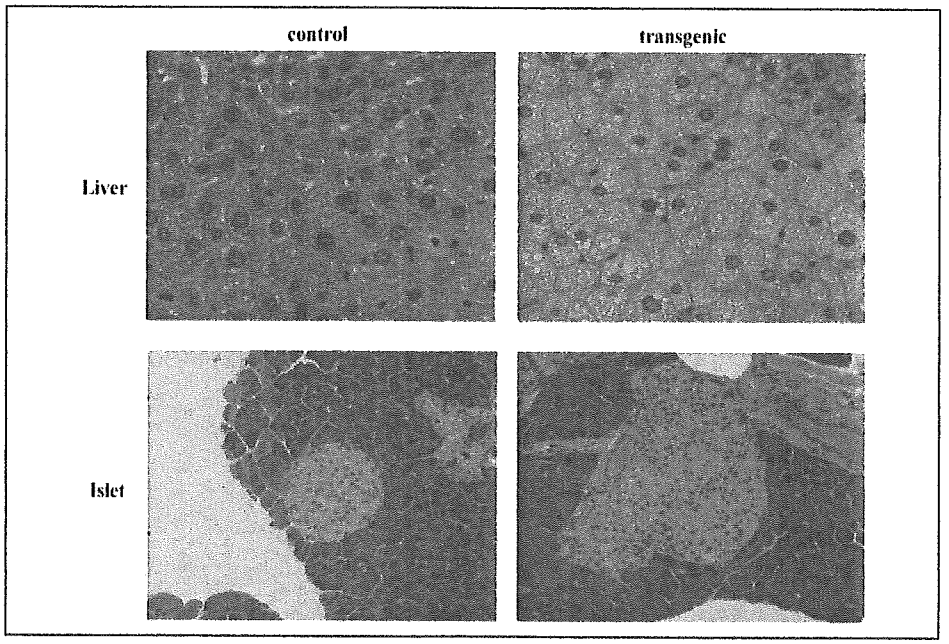

FIGURE 4. **Liver and pancreatic islet histologies in 16-week-old line 1 RELMβ transgenic and control mice that had been fed a high fat diet for 4 weeks.** Liver and pancreatic sections from adult, high fat diet fed mice were stained with hematoxylin and eosin. The mean islet area is presented in TABLE TWO.

the levels of serum free fatty acid and adiponectin were not altered (n = 8–10).

Histological Analysis of Liver and Pancreas—Histology showed fatty liver and islet hyperplasia in transgenic mice as compared with control mice (n = 3, age 16 weeks, after 4 weeks on a high fat diet, Fig. 4). Quantitatively, the mean islet area in RELMβ-overexpressing mice was significantly increased, as compared with that in control mice, by approximately 2.5-fold (TABLE TWO). In contrast, no significant difference in adipocyte size or mass was seen in epididymal or subcutaneous fat at the time of sacrifice (data not shown).

Glucose Clamp Study and Glucose Uptake in Vivo and in Vitro—Six-month-old mice fed a high fat diet for 4 weeks were used for the glucose clamp study. In the basal state, glucose levels were 113.3 ± 2.0 *versus* 158 ± 9.5 mg/dl (control *versus* transgenic), and insulin levels were 5.0 ± 1.2 *versus* 12.1 ± 5.4 ng/ml. There was no significant difference in either glucose utilization or hepatic glucose output (Fig. 5, *b* and *c*). In the hyperinsulinemic euglycemic clamp study, glucose levels were 96.0 ± 5.3 *versus* 100.8 ± 5.3 mg/dl, and insulin levels were 20.3 ± 5.2 *versus* 22.4 ± 2.8 ng/ml. RELMβ transgenic mice showed a 35% lower glucose infusion rate (Fig. 5*a*) due to markedly insufficient suppression of hepatic glucose output, (about one-fifth of the expected suppression, Fig. 5*c*), whereas hyperinsulinemia had no effect on the glucose disappearance rate (Fig. 5*b*).

We found no significant difference in glucose uptake *in vivo* during the clamp by either muscles or fat (Fig. 5*d*), nor in insulin stimulated glucose uptake *in vitro* by isolated soleus muscle between RELMβ-overexpressing mice and their littermates, at 3 months of age after 4 weeks on a high fat diet, *i.e.* immediately before the experiment (Fig. 5*e*).

Insulin Signaling in RELMβ Transgenic Mice—To reveal the mechanism of glucose intolerance in the RELMβ transgenic mice, we investi-

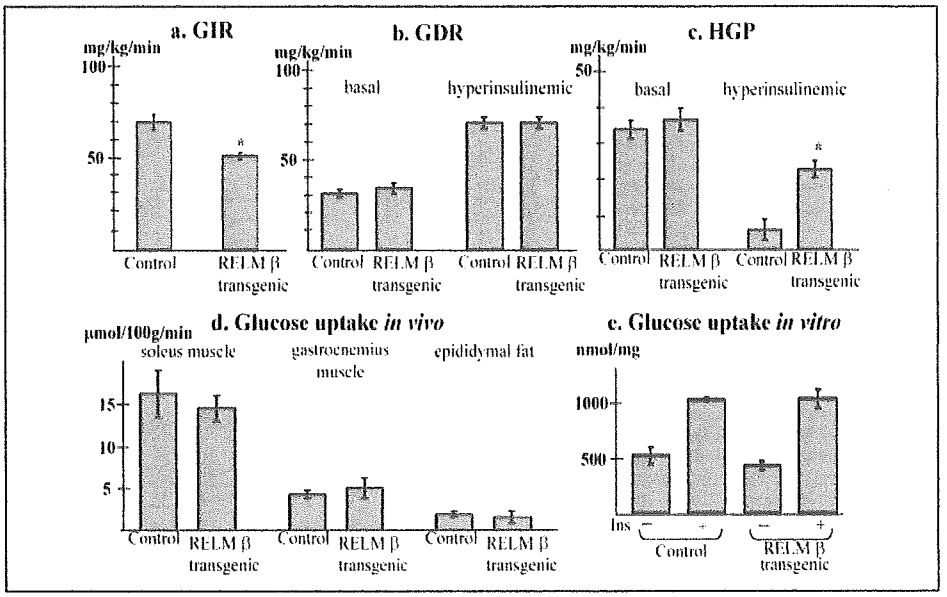

FIGURE 5. *a–d*, glucose clamp study of RELMβ overexpressing line 1 at 6 months of age, following 4 weeks of being fed a high fat diet. Blood samples were collected every 30 min to determine the glucose specific activity and blood glucose and plasma insulin concentration during 90-min basal period and 150-min clamp period. At the end of the study, tissues were sampled for determination of tissue glucose uptake rates during the clamp period. *a*, glucose infusion rate in the hyperinsulinemic euglycemic state. *b*, glucose disposal rates in basal and hyperinsulinemic states. *c*, glucose production rate in basal and hyperinsulinemic states. *d*, glucose uptake by soleus muscle, gastrocnemius muscle, and epididymal fat *in vivo*. *e*, glucose uptake by isolated soleus muscle *in vitro*. −, without insulin stimulation; +, with insulin stimulation. Values are presented as means ± S.E. In *b–e*, statistical analysis was performed using two-way analysis of variance. Statistical significance is indicated by an *asterisk*: *, $p < 0.05$ for RELMβ transgenic mice *versus* control age-matched mice.

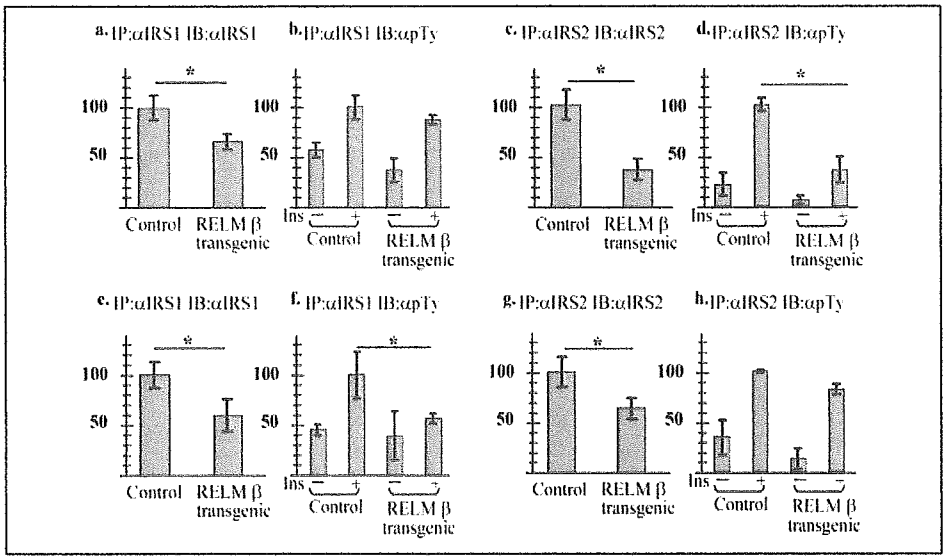

FIGURE 6. **The protein contents and phosphorylations of IRS-1/2 in liver (*a–d*) and muscle (*e–h*) from 3-month-old RELMβ-overexpressing line 1 mice, which had been fed a high fat diet for 4 weeks.** Values are presented as means ± S.E. −, without insulin stimulation; +, with insulin stimulation. The *scale* represents the percentage of control (with insulin stimulation, if performed). Statistical significance is indicated by an *asterisk*: *, $p < 0.05$ for control mice *versus* transgenic mice.

gated protein contents, phosphorylations, and insulin signaling cascade activity using the highly RELMβ-overexpressing (*line 1*, Fig. 1*b*) line 1 3-month old mice, which had been fed a high fat diet for 4 weeks. We found that IRS-1 and IRS-2 protein contents were significantly decreased in the livers and muscles of transgenic mice (IRS-1: 34% decrease in liver, 40% in muscle, $p < 0.05$; IRS-2: 64% in liver and 36% in muscle, $p < 0.05$) (Fig. 6, *a*, *c*, *e*, and *g*). The insulin-induced tyrosine phosphorylations of IRS-1 and IRS-2 were also decreased in the livers and muscles of transgenic mice (Fig. 6, *b*, *d*, *f*, and *h*). In the liver, the decrease in IRS-2 phosphorylation ($p < 0.05$) was more evident than that of IRS-1, whereas the IRS-1 decrease was more evident in muscle. Similarly, the PI 3-kinase activities associated with IRS-1 and IRS-2 in response to insulin stimulation were significantly suppressed, by ~40%, in transgenic mice (Fig. 7, *a–e*). Finally, Akt kinase activity in the presence of insulin stimulation was also decreased in both liver (40%) and muscle (35%) in transgenic mice (Fig. 8, *a–e*), whereas Akt protein contents were not significantly altered.

RELMβ Activates ERK, p38, and JNK while Suppressing Insulin Signaling in Primary Cultured Hepatocytes—To investigate the effects of RELMβ on insulin signaling in the liver, primary cultured hepatocytes were prepared. The treatment of hepatocytes with 1 μg/ml of recombinant RELMβ for 24 h induced apparent decreases in both IRS-1 (70% $p < 0.005$) and IRS-2 (49%, $p < 0.005$) protein contents (Fig. 9, *a* and *b*). Similarly, insulin-stimulated phosphorylations of IRS-1 and IRS-2 were also suppressed by treatment with RELMβ (Fig. 9, *c* and *d*). Subsequently, mRNA levels of gluconeogenetic enzymes, glucose-6-phosphatase, and phosphoenolpyruvate carboxylase kinase were elevated (Fig. 9, *e* and *f*). This suggested RELMβ to directly produce insulin resistance in the liver.

Next, to reveal the molecular mechanism underlying the suppressed expression and phosphorylation of IRS-1 and IRS-2, we studied the effects of RELMβ on the three MAPKs, ERK, p38, and SAPK/JNK, all of which can reportedly induce insulin resistance. Hepatocytes were treated with 1 μg/ml RELMβ or 10 ng/ml tumor necrosis factor α for 10 or 30 min, and the phosphorylations of ERK,

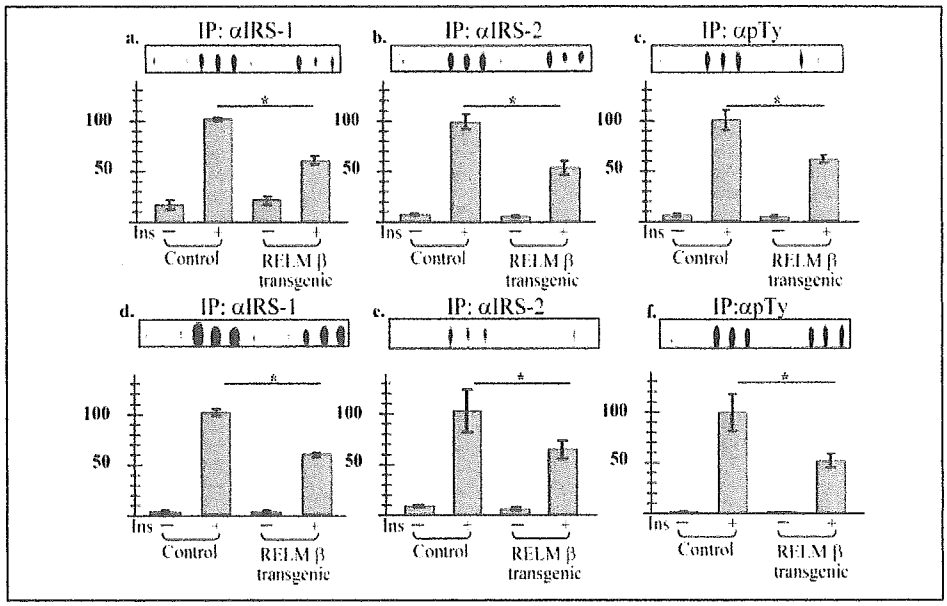

FIGURE 7. **Insulin-induced PI 3-kinase activation in 3-month-old line 1 RELMβ transgenic and control mice that had been fed a high fat diet for 4 weeks.** *a–c*, phosphorylation of PI was carried out in immune complexes from the liver lysate. *a–c*, are IRS-1-, IRS-2-, and pTy-associated PI 3-kinase activities, respectively. *d–f*, phosphorylation of PI was carried out in immune complexes from the muscle lysate. *d–f*, are IRS-1-, IRS-2-, and pTy-associated PI3K activities, respectively. *Lower portions* of the *upper panels* show the autoradiographic results of the PI 3-kinase assay, and means ± S.E. values are presented in the *lower panels*. −, without insulin stimulation; +, with insulin stimulation. The *scale* represents the percentage of control with insulin stimulation. Statistical significance is indicated by an *asterisk*: *, $p < 0.05$ for control mice *versus* transgenic mice.

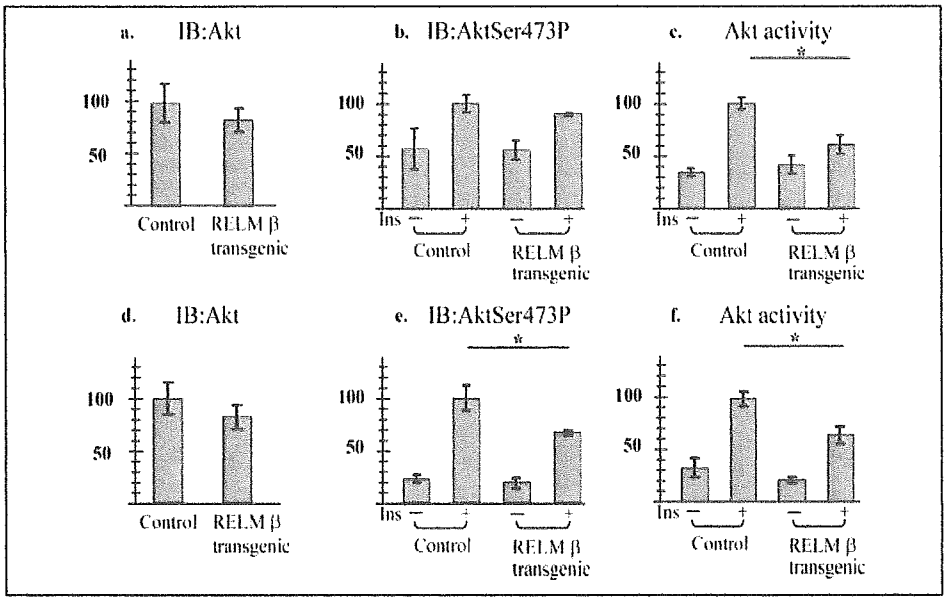

FIGURE 8. **The protein contents, phosphorylation of Akt, and Akt activity in liver (*a–c*) and muscle (*d–f*) from 3-month-old RELMβ-overexpressing line 1 mice, which had been fed a high fat diet for 4 weeks.** Values are presented as means ± S.E. −, without insulin stimulation; +, with insulin stimulation. The *scale* represents the percentage of control (with insulin stimulation, if performed). Statistical significance is indicated by an *asterisk*: *, $p < 0.05$ for control mice *versus* transgenic mice.

p38, and JNK were assessed by immunoblotting with the antibodies to detect phosphorylation of p44/p42 (ERK1/2), p38 MAPK, and p54/p46 (SAPK/JNK). RELMβ was revealed to markedly phosphorylate ERK and p38, but JNK only weakly (*left side* of Fig. 10, *a* and *c*). The phosphorylations induced by RELMβ were more intense 30 min after the initiation of stimulation than at 10 min, whereas tumor necrosis factor α-induced phosphorylations of MAPKs were shown to peak at ~10 min (*right side* of Fig. 10*a*). The effect of RELMβ was concentration-dependent, and as little as 10 ng/ml RELMβ stimulated all three MAPKs (Fig. 10, *b* and *d*). In addition, increased phosphorylation of p38 was observed in both the liver and muscle of RELMβ transgenic mice (Fig 11) in the basal, *i.e.* fasted, state, although there were no significant changes in the phosphorylations of ERK and JNK.

Key Enzymes for Lipid Metabolism Showed Modestly Altered Transcriptional Levels in RELMβ Transgenic Mice—To investigate the mechanisms of hyperlipidemia in RELMβ transgenic mice, mRNA levels of key lipid metabolic enzymes were evaluated using a RELMβ-overexpressing line (*line 1*) *i.e.* 3-month-old mice that had been fed a high fat diet for 4 weeks. A lipogenic enzyme (fatty acid synthase, 60%) was increased and lipolytic enzymes (carnitine palmitoyltransferase-1, 32%, PPARα: peroxisome proliferator activated receptor-α, 33%) were decreased (TABLE THREE). These changes probably contribute to the mechanisms underlying the moderate hyperlipidemia in RELMβ-overexpressing mice.

DISCUSSION

Although the gut is the site of nutrient absorption, the gastrointestinal tract secretes several hormones such as glucagon-like peptide-1, gastric inhibitory polypeptide, and ghrelin. These hormones reportedly influence metabolic conditions by regulating insulin secretion and appetite (28–31). Recently, two RELMs were also identified as hormones secreted from the mouse small intestine and colon (9, 10), and we previously reported that these gut-derived RELMs are apparently up-

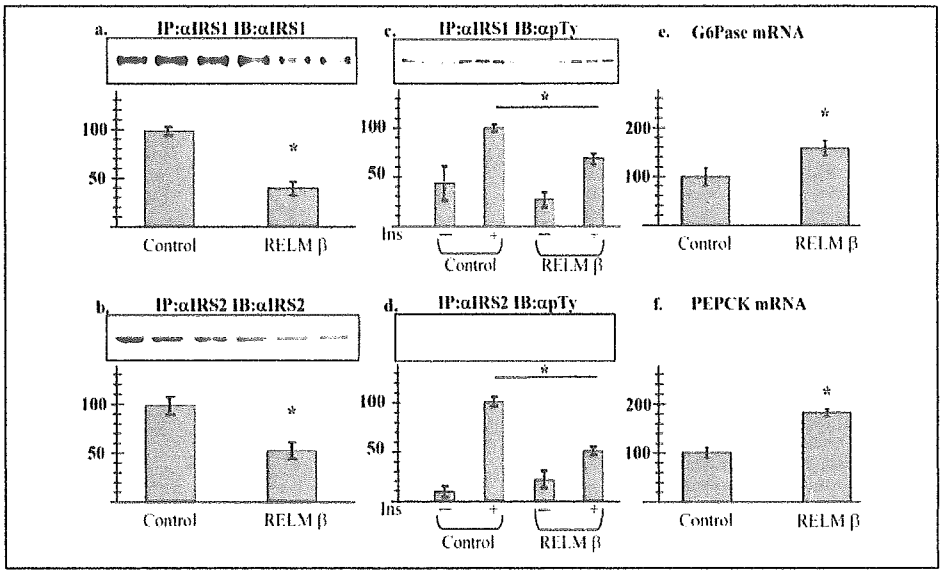

FIGURE 9. **IRS-1 and IRS-2 protein contents and phosphorylation by insulin in primary culture of hepatocytes, and mRNA levels of glucose-6-phosphatase and phosphoenolpyruvate carboxylase kinase.** Values are presented as means ± S.E. (*a*) and (*b*) compare the IRS protein contents. In *c* and *d*, phosphorylation of IRS; −, without insulin stimulation; +, with insulin stimulation. mRNA amount of glucose-6-phosphatase (*e*) and mRNA amount of phosphoenolpyruvate carboxylase kinase (*f*) are corrected by actin mRNA amount as the internal control; *scale* represents the percentage of control (without RELMβ). *, $p < 0.05$ for the condition without RELMβ (*Control*) *versus* with RELMβ (*RELMβ*). Each experiment was performed at least three times.

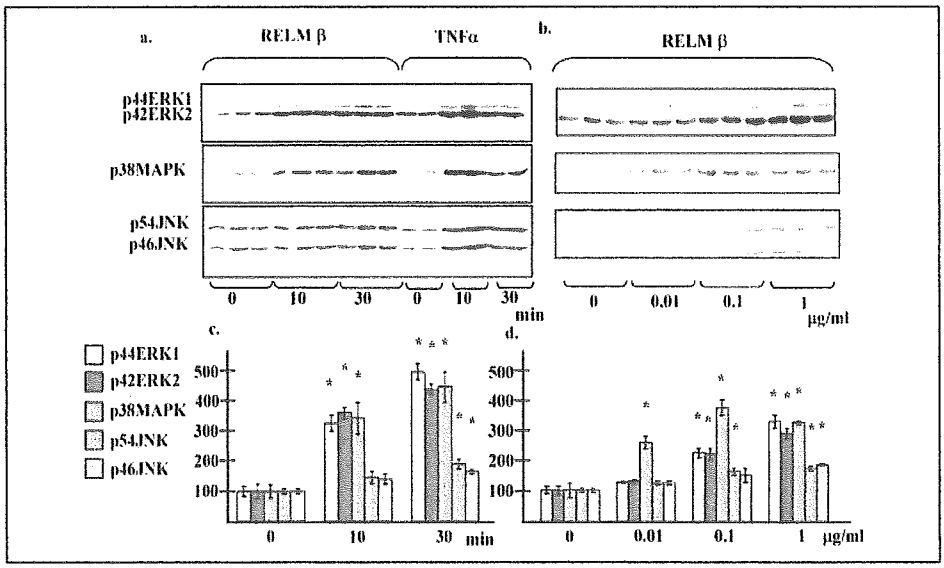

FIGURE 10. **MAPK phosphorylations in response to RELMβ stimulation in primary hepatocytes.** Western blots for phosho-p44/p42(ERK1/2), phospho-p38, and phospho-p54/p46(SAPK/JNK) were performed with: *a*, 10 or 30 min of RELMβ and tumor necrosis factor α stimulation; *b*, 0.01, 0.1, or 1 μl/ml RELMβ stimulation; *c*, densitometry of *a*; *d*, densitometry of *b*. Values are presented as means ± S.E. Each condition was examined 3–6 times. The *scale* represents the percentage of control. Statistical significance is indicated by an *asterisk*: *, $p < 0.05$ for the condition without RELMβ (*Control*) *versus* with RELMβ (*RELMβ*).

regulated in insulin-resistant rodent models. Thus, we speculated that the gastrointestinal tract might regulate insulin sensitivity by secreting these RELMs into the circulation in response to intestinal circumstances, *i.e.* inflammation, the food intake amount, and/or the nutritional contents of the food. Based on this hypothesis, this study was designed to answer questions as to whether or not the increased expression of gut-derived RELMβ actually induces insulin resistance, and if so, what molecular mechanisms underlie this regulation. To answer these questions, we generated transgenic mice with hepatic RELMβ overexpression, because overexpression in the liver is a commonly used method of investigating the chronic functions of several hormones, including leptin, growth hormone, and so on.

We speculate that RELMβ might possess dual roles; one in the circulation and the other in the gut. RELMβ functioning in the gut would be excreted into the stool. We consider hepatic RELMβ-overexpressing mice to be useful for investigating the role of RELMβ in the circulation, because overexpressing RELMβ in the liver, assuming a high focal concentration, would mimic the physiological pattern of RELMβ concentrations, because RELMβ probably initially flows into the liver via the portal vein.

We first demonstrated both line 1 and line 2 RELMβ transgenic mice, on a high fat diet, to phenotypically show hyperglycemia, hyperlipidemia, and hyperinsulinemia. Taking the data for line 2 into consideration, it seems that a relatively small increase in RELMβ expression can induce significant insulin resistance, which suggests that the increased serum RELMβ concentrations observed in the insulin resistant rodent models are physiologically significant. The consequent islet hyperplasia was considered to be due to prolonged insulin resistance. However, on the other hand, it should be noted that, when the mice were fed a normal diet, these metabolic abnormalities did not become overt even in the highly RELMβ-overexpressing line (line 1). This finding suggests that RELMβ itself induces a limited degree of insulin resistance that is not sufficient to cause overt diabetes or hyperlipidemia. Some additional factor(s) causing insulin resistance (in the case of our experiments, the high fat diet feeding) in addition to the increased serum RELMβ concentration would be necessary to induce diabetes or hyperlipidemia. It is also reasonable to regard increased RELMβ expression as just one of several independent molecular mechanisms underlying high fat diet insulin resistance.

Next, we demonstrated the presence of hepatic insulin resistance in

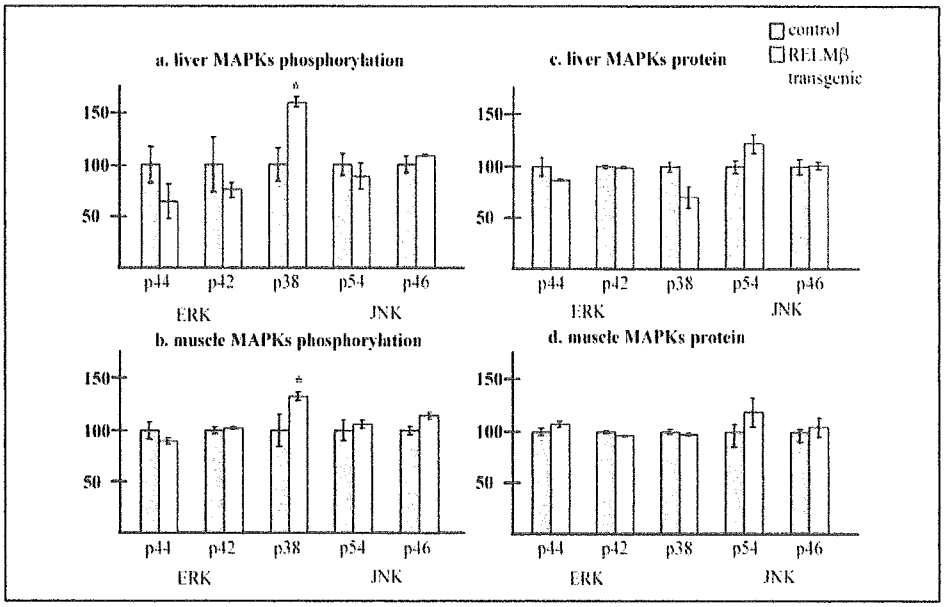

FIGURE 11. **MAPK phosphorylations and protein levels from 3-month-old RELMβ-overexpressing line 1 mice that had been fed a high fat diet, after an overnight fast.** Western blots for phosho-p44/p42(ERK1/2), p44/42, phospho-p38, p38, phospho-p54/p46(SAPK/JNK), and p54/p46 were performed. Each condition was examined in triplicate. The *scale* represents the percentage of control. Statistical significance is indicated by an *asterisk*: *, $p < 0.05$ for control mice *versus* transgenic mice.

TABLE THREE

mRNA levels of key lipid metabolic enzymes in the liver, measured using ribonuclease protection assay (RPA) using RELMβ overexpressing line 1 mice, at the age of 3 months, which had been fed a high fat diet for 4 weeks

Values are corrected by actin mRNA levels and by mean values of control mice as the standard (1.00 as standard mean value).

	Control	RELMβ trangenic
LDLR	1.00 ± 0.09	1.02 ± 0.06
PPARα	1.00 ± 0.13	0.72 ± 0.03
CPT1	1.00 ± 0.07	0.77 ± 0.07[a]
SREBP-1a	1.00 ± 0.08	0.98 ± 0.08
SREBP-1c	1.00 ± 0.17	0.92 ± 0.08
ACC	1.00 ± 0.04	1.09 ± 0.01[a]
FAS	1.00 ± 0.09	1.60 ± 0.34[a]
SCD1	1.00 ± 0.20	1.03 ± 0.15

[a] $p < 0.05$.

RELMβ transgenic mice, maintained on a high fat diet, by hyperinsulinemic glucose clamp test, which showed markedly increased hepatic glucose output while glucose utilization was intact. The pyruvate tolerance test, which reflects hepatic gluconeogenesis, yielded complementary results, because pyruvate is a substrate for gluconeogenesis (17). In contrast, we did not find changes in insulin-induced glucose transport activity in either peripheral tissues *in vivo*, or in isolated skeletal muscles *in vitro* from RELMβ transgenic as compared with control mice. Indeed, histochemical analysis revealed fatty livers in the RELMβ transgenic mice, although there was no obvious obesity at the time of sacrifice. Thus, it seems that glucose intolerance and hyperlipidemia in RELMβ transgenic mice are attributable mainly to hepatic insulin resistance. There is a curious discrepancy between the apparent insulin resistance in the insulin signaling pathway (*e.g.* insulin-induced PI 3-kinase activity) and unchanged insulin-induced glucose uptake by muscle, suggesting one or more compensatory mechanisms involving insulin-induced glucose transport, although this remains entirely speculative. In view of organ cross-talk, primary hepatic insulin resistance might affect glucose uptake in other peripheral tissues.

Subsequently, to elucidate whether or not the contribution of RELMβ to hepatic insulin resistance is direct, and what changes in signal transduction are induced by RELMβ, we performed experiments using primary cultured hepatocytes. Importantly, the expressions of IRS-1 and IRS-2 were demonstrated to be down-regulated in RELMβ-treated hepatocytes as well as liver and muscle tissues from RELMβ transgenic mice. In good agreement with the decreased IRS-1 and IRS-2 contents, PI 3-kinase activities associated with IRS-1 and IRS-2 and Akt activation, which are reportedly essential for insulin-induced metabolic actions, were also attenuated. These findings suggest that RELMβ functions directly in insulin-sensitive cells such as hepatocytes to suppress insulin signaling rather than as a consequence of hepatic lipid accumulation or of altered functions of other tissues such as adipose. The pattern of change in IRS protein contents is similar to that of *ob/ob* mice (32). Given the elevated serum concentration of RELMβ in the *ob/ob* mice, it may be reasonable to consider the elevated serum RELMβ concentration to at least contribute to the decreased IRS-1 and IRS-2 contents.

The next question concerns which type of signal transduction induced by RELMβ is involved in suppressing insulin signaling. Several previous studies have confirmed that the activation of ERK-1/2 or p38 MAPK leads to down-regulation of IRS-1 and IRS-2 (26). The activated JNK reportedly phosphorylates the serine residue in IRS-1 and suppresses insulin-induced PI 3-kinase activation. Thus, we investigated the effect of RELMβ on MAPK signaling using primary cultured hepatocytes. We found that ERK1/2, p38, and SAPK/JNK are phosphorylated in response to RELMβ. It was also recently reported that resistin phosphorylates and activates ERK-1/2 and p38 in smooth muscle cells (33). Thus, resistin and RELMβ are likely to have the same function. In addition, a significant increase in p38, but not ERK or JNK, phosphorylation was observed in both liver and muscle tissues of RELMβ transgenic mice. Because stimulation with RELMβ is constitutive in transgenic mice, we speculated that the effect of RELMβ might be difficult to detect but our results were consistent with those obtained using primary cultured hepatocytes.

Lipid metabolism remains an important issue. Some hepatic lipolytic and lipogenic enzymes were altered to promote lipid accumulation in the liver. These modest changes apparently reflect the moderate hyperlipidemia and liver steatosis of RELMβ transgenic mice. However, it is noteworthy that the key transcriptional factor, SREBP-1c, regulating lipid synthesis was not altered. The activation of p38 and other MAPKs

by RELMβ may be involved in regulating lipid metabolism as previously reported (34–36).

Our results suggest that chronic stimulation by RELMβ causes glucose intolerance and hyperlipidemia associated with impaired insulin signaling, and the activations of three MAPKs are probably involved in this insulin signaling suppression. Although our findings suggest the importance of increased RELMβ expression in the pathogenesis of diabetes and hyperlipidemia, there are still limitations in interpreting the physiological role of RELMβ in the pathogenesis of insulin resistance, because glucose homeostasis is modestly impaired in RELMβ transgenic mice relative to control mice, on a high fat diet only. Thus, further studies are necessary to elucidate how much RELMβ actually contributes to insulin resistance caused by various factors. For example, the percentages of RELMβ present in circulating blood as monomers, dimers, and hexamers and the biological activities of each form, should be determined. Identification of the specific RELMβ receptor as well as the relationship between serum RELMβ and insulin sensitivity in humans are important. Further studies may reveal that RELMβ is a potentially useful marker for assessing insulin resistance associated with obesity and may serve as a target for novel anti-diabetic agents.

REFERENCES

1. Steppan, C. M., Bailey, S. T., Bhat, S., Brown, E. J., Banerjee, R. R., Wright, C. M., Patel, H. R., Ahima, R. S., and Lazar, M. A. (2001) *Nature* **409,** 307–312
2. Kim, K. H., Lee, K., Moon, Y. S., and Sul, H. S. (2001) *J. Biol. Chem.* **276,** 11252–11256
3. Moon, B., Kwan, J. J., Duddy, N., Sweeney, G., and Begum, N. (2003) *Am. J. Phys-iol.* **285,** E106–E115
4. Banerjee, R. R., Rangwala, S. M., Shapiro, J. S., Rich, A. S., Rhoades, B., Qi, Y., Wang, J., Rajala, M. W., Pocai, A., Scherer, P. E., Steppan, C. M., Ahima, R. S., Obici, S., Rossetti, L., and Lazar, M. A. (2004) *Science.* **303,** 1195–1198
5. Rangwala, S. M., Rich, A. S., Rhoades, B., Shapiro, J. S., Obici, S., Rossetti, L., and Lazar, M. A. (2004) *Diabetes* **53,** 1937–1941
6. Satoh, H., Nguyen, M. T., Miles, P. D., Imamura, T., Usui, I., and Olefsky, J. M. (2004) *J. Clin. Invest.* **114,** 224–231
7. Fehmann, H. C., and Heyn, J. (2002) *Horm. Metab. Res.* **34,** 671–673
8. Lee, J. H., Chan, J. L., Yiannakouris, N., Kontogianni, M., Estrada, E., Seip, R., Orlova, C., and Mantzoros, C. S. (2003) *J. Clin. Endocrinol. Metab.* **88,** 4848–4856
9. Steppan, C. M., Brown, E. J., Wright, C. M., Bhat, S., Banerjee, R. R., Dai, C. Y., Enders, G. H., Silberg, D. G., Wen, X., Wu, G. D., and Lazar, M. A. (2001) *Proc. Natl. Acad. Sci. U. S. A.* **98,** 502–506
10. Chumakov, A. M., Kubota, T., Walter, S., and Koeffler, H. P. (2004) *Oncogene* **23,** 3414–3425
11. Rajala, M. W., Obici, S., Scherer, P. E., and Rossetti, L. (2003) *J. Clin. Invest.* **111,** 225–230
12. Shojima, N., Ogihara, T., Inukai, K., Fujishiro, M., Sakoda, H., Kushiyama, A., Katagiri, H., Anai, M., Ono, H., Fukushima, Y., Horike, N., Viana, A. Y., Uchijima, Y., Kurihara, H., and Asano, T. (2005) *Diabetologia* **48,** 984–992
13. Ono, H., Shimano, H., Katagiri, H., Yahagi, N., Sakoda, H., Onishi, Y., Anai, M., Ogihara, T., Fujishiro, M., Viana, A. Y., Fukushima, Y., Abe, M., Shojima, N., Kikuchi, M., Yamada, N., Oka, Y., and Asano, T. (2003) *Diabetes* **52,** 2905–2913
14. Anai, M., Funaki, M., Ogihara, T., Kanda, A., Onishi, Y., Sakoda, H., Inukai, K., Nawano, M., Fukushima, Y., Yazaki, Y., Kikuchi, M., Oka, Y., and Asano, T. (1999) *Diabetes* **48,** 158–169
15. Folch, J., Lees, M., and Sloane Stanley, G. H. (1957) *J. Biol. Chem.* **226,** 497–509
16. Bergmeyer, H., Bergmeyer, J., and Grassl, M. (1984) *Methods of Enzymatic Analys-is, 3rd ed.*, Wiley, Hoboken, NJ, pp. 11–18
17. Miyake, K., Ogawa, W., Matsumoto, M., Nakamura, T., Sakaue, H., and Kasuga, M. (2002) *J. Clin. Invest.* **110,** 1483–1491
18. Onishi, Y., Honda, M., Ogihara, T., Sakoda, H., Anai, M., Fujishiro, M., Ono, H., Shojima, N., Fukushima, Y., Inukai, K., Katagiri, H., Kikuchi, M., Oka, Y., and Asano, T. (2003) *Biochem. Biophys-. Res. Commun.* **303,** 788–794
19. Miles, P. D., Barak, Y., Evans, R. M., and Olefsky, J. M. (2003) *Am. J. Phys-iol.* **284,** E618–E626
20. Fueger, P. T., Bracy, D. P., Malabanan, C. M., Pencek, R. R., Granner, D. K., and Wasserman, D. H. (2004) *Diabetes* **53** 306–314
21. Fisher, S. J., and Kahn, C. R. (2003) *J. Clin. Invest.* **111,** 463–468
22. Ogihara, T., Shin, B. C., Anai, M., Katagiri, H., Inukai, K., Funaki, M., Fukushima, Y., Ishihara, H., Takata, K., Kikuchi, M., Yazaki, Y., Oka, Y., and Asano, T. (1997) *J. Biol. Chem.* **272,** 12868–12873
23. Ogihara, T., Asano, T., Katagiri, H., Sakoda, H., Anai, M., Shojima, N., Ono, H., Fujishiro, M., Kushiyama, A., Fukushima, Y., Kikuchi, M., Noguchi, N., Aburatani, H., Gotoh, Y., Komuro, I., and Fujita, T. (2004) *Diabetologia* **47,** 794–805
24. Sakoda, H., Ogihara, T., Anai, M., Fujishiro, M., Ono, H., Onishi, Y., Katagiri, H., Abe, M., Fukushima, Y., Shojima, N., Inukai, K., Kikuchi, M., Oka, Y., and Asano, T. (2002) *Am. J. Phys-iol.* **282,** E1239–E1244
25. Sakoda, H., Gotoh, Y., Katagiri, H., Kurokawa, M., Ono, H., Onishi, Y., Anai, M., Ogihara, T., Fujishiro, M., Fukushima, Y., Abe, M., Shojima, N., Kikuchi, M., Oka, Y., Hirai, H., and Asano, T. (2003) *J. Biol. Chem.* **278,** 25802–25807
26. Fujishiro, M., Gotoh, Y., Katagiri, H., Sakoda, H., Ogihara, T., Anai, M., Onishi, Y., Ono, H., Abe, M., Shojima, N., Fukushima, Y., Kikuchi, M., Oka, Y., and Asano, T. (2003) *Mol. Endocrinol.* **17,** 487–497
27. Tomimoto, S., Hashimoto, H., Shintani, N., Yamamoto, K., Kawabata, Y., Hamagami, K., Yamagata, K., Miyagawa, J., and Baba, A. (2004) *J. Pharmacol. Exp. Ther.* **309,** 796–803
28. Kojima, M., Hosoda, H., Date, Y., Nakazato, M., Matsuo, H., and Kangawa, K. (1999) *Nature.* **402,** 656–660
29. Miyawaki, K., Yamada, Y., Yano, H., Niwa, H., Ban, N., Ihara, Y., Kubota, A., Fujimoto, S., Kajikawa, M., Kuroe, A., Tsuda, K., Hashimoto, H., Yamashita, T., Jomori, T., Tashiro, F., Miyazaki, J., and Seino, Y. (1999) *Proc. Natl. Acad. Sci. U. S. A.* **96,** 14843–14847
30. Murata, M., Okimura, Y., Iida, K., Matsumoto, M., Sowa, H., Kaji, H., Kojima, M., Kangawa, K., and Chihara, K. (2002) *J. Biol. Chem.* **277,** 5667–5674
31. Mooney, M. H., Abdel-Wahab, Y. H., McKillop, A. M., O'Harte, F. P., and Flatt, P. R. (2002) *Biochim. Biophys-. Acta* **1569,** 75–80
32. Kerouz, N. J., Horsch, D., Pons, S., and Kahn, C. R. (1997) *J. Clin. Invest.* **100,** 3164–3172
33. Calabro, P., Samudio, I., Willerson, J. T., and Yeh, E. T. (2004) *Circulation* **110,** 3335–3340
34. Samuel, V. T., Liu, Z. X., Qu, X., Elder, B. D., Bilz, S., Befroy, D., Romanelli, A. J., and Shulman, G. I. (2004) *J. Biol. Chem.* **279,** 32345–32353
35. Mehta, K. D., and Miller, L. (1999) *Trends Cardiovasc. Med.* **9,** 201–205
36. Kapoor, G. S., Atkins, B. A., and Mehta, K. D. (2002) *Mol. Cell Biochem.* **236,** 13–22

THE JOURNAL OF BIOLOGICAL CHEMISTRY VOL. 280, NO. 47, pp. 39609–39615, November 25, 2005

WFS1 Is a Novel Component of the Unfolded Protein Response and Maintains Homeostasis of the Endoplasmic Reticulum in Pancreatic β-Cells*

Received for publication, July 8, 2005, and in revised form, September 27, 2005 Published, JBC Papers in Press, September 29, 2005, DOI 10.1074/jbc.M507426200

Sonya G. Fonseca[‡], Mariko Fukuma[‡1], Kathryn L. Lipson[‡], Linh X. Nguyen[‡], Jenny R. Allen[‡], Yoshitomo Oka[§], and Fumihiko Urano[‡¶2]

From the [‡]Program in Gene Function and Expression and [¶]Program in Molecular Medicine, University of Massachusetts Medical School, Worcester, Massachusetts 01605 and [§]Division of Molecular Metabolism and Diabetes, Tohoku University Graduate School of Medicine, Sendai 980-8575, Japan

In Wolfram syndrome, a rare form of juvenile diabetes, pancreatic β-cell death is not accompanied by an autoimmune response. Although it has been reported that mutations in the *WFS1* gene are responsible for the development of this syndrome, the precise molecular mechanisms underlying β-cell death caused by the *WFS1* mutations remain unknown. Here we report that WFS1 is a novel component of the unfolded protein response and has an important function in maintaining homeostasis of the endoplasmic reticulum (ER) in pancreatic β-cells. WFS1 encodes a transmembrane glycoprotein in the ER. WFS1 mRNA and protein are induced by ER stress. The expression of WFS1 is regulated by inositol requiring 1 and PKR-like ER kinase, central regulators of the unfolded protein response. WFS1 is normally up-regulated during insulin secretion, whereas inactivation of WFS1 in β-cells causes ER stress and β-cell dysfunction. These results indicate that the pathogenesis of Wolfram syndrome involves chronic ER stress in pancreatic β-cells caused by the loss of function of WFS1.

In 1938, Wolfram and Wagener (1) analyzed four siblings with the combination of juvenile diabetes and optic atrophy, thus providing the first report of Wolfram syndrome. Because a significant portion of patients with Wolfram syndrome develop diabetes insipidus and auditory nerve deafness, this syndrome is also referred to as the diabetes insipidus, diabetes mellitus, optic atrophy, and deafness syndrome (2, 3). Its pathogenesis is still unknown.

Although patients with Wolfram syndrome are not generally obese and do not have insulitis, the β-cells in their pancreatic islets are selectively destroyed (4). Families that exhibit Wolfram syndrome share mutations in a gene encoding the WFS1 protein, a transmembrane protein in the endoplasmic reticulum (ER)[3] (5, 6). WFS1 serves as an ER calcium channel (7), suggesting that this molecule may have a function in ER homeostasis. Therefore, inactivation of WFS1 may cause imbalances in ER homeostasis.

The ER is an important cellular compartment for the folding of newly synthesized secretory proteins such as proinsulin. Imbalance in ER homeostasis elicits stress in this organelle. ER stress is defined as an imbalance between the actual folding capacity of the ER and the demand placed on this organelle. The unfolded protein response (UPR), an adaptive response that counteracts ER stress, has three components as follows: gene expression, translational attenuation, and ER-associated protein degradation system (8–10). Accumulating evidence suggests that a high level of ER stress or defective ER stress signaling (*i.e.* the UPR) causes β-cell death during the development of diabetes (9, 11–13).

Inositol requiring 1 (IRE1), a sensor for unfolded and misfolded proteins in the ER, is a central regulator of the UPR. IRE1α, which is expressed ubiquitously, has a high level of expression in the pancreas and placenta (14, 15); IRE1β is expressed only in epithelial cells of the gastrointestinal tract (16, 17). The presence of unfolded proteins in the ER causes dimerization, trans-autophosphorylation, and consequent activation of IRE1. Activated IRE1 splices XBP-1 (X-box binding protein-1) mRNA, leading to synthesis of the active transcription factor XBP-1 and up-regulation of UPR genes (18, 19). In contrast, prolonged ER stress activates the cell-death pathway through IRE1. Under chronic ER stress, IRE1 recruits tumor necrosis factor receptor-associated factor 2 (20), which activates apoptosis-signaling kinase 1 (ASK1) (21, 22). Activated ASK1 leads to the activation of c-Jun N-terminal protein kinase and, in the presence of extreme ER stress, induces apoptosis (23). It has been suggested that this pathway is important for insulin resistance in patients with type 2 diabetes (24). Obesity causes ER stress in the liver and leads to hyperactivation of c-Jun N-terminal protein kinase signaling. This causes serine phosphorylation of insulin receptor substrate-1 and inhibits insulin action in liver cells. In addition, tumor necrosis factor receptor-associated factor 2 recruitment by IRE1 causes clustering and activation of caspase-12 at the ER membrane (25). Activated caspase-12 induces apoptosis under pathological ER stress conditions (26).

Two more upstream components in the UPR, PKR-like ER kinase (PERK) and activating transcription factor 6 (ATF6) (27–29), are also sensors of unfolded or misfolded proteins and are activated by the accumulation of such proteins in the ER. PERK is highly expressed in pancreatic islets (29, 30). Activated PERK phosphorylates the α subunit of eukaryotic translation initiation factor 2 (eIF2α), which leads to the attenuation of general protein translation. This reduces the ER workload and protects cells from apoptosis resulting from ER stress (31). In Wolcott-Rallison syndrome, a rare form of juvenile diabetes, mutations

* This work was supported by NIDDK Grant 1R01DK067493-01 from the National Institutes of Health, the National Institutes of Health Diabetes and Endocrinology Research Center at the University of Massachusetts Medical School, a Worcester Foundation award, a Juvenile Diabetes Research Foundation Innovative grant, an American Diabetes Association Innovation grant, and an Iacocca Foundation grant (to F. U.). The costs of publication of this article were defrayed in part by the payment of page charges. This article must therefore be hereby marked "*advertisement*" in accordance with 18 U.S.C. Section 1734 solely to indicate this fact.

[1] Present address: Dept. of Pathology, Keio University School of Medicine, Tokyo 160-8582, Japan.

[2] To whom correspondence should be addressed: Program in Gene Function and Expression, University of Massachusetts Medical School, Worcester, MA 01605-2324. Tel.: 508-856-6012; Fax: 508-856-4650; E-mail: Fumihiko.Urano@umassmed.edu.

[3] The abbreviations used are: ER, endoplasmic reticulum; UPR, unfolded protein response; IRE1, inositol requiring 1; PERK, PKR-like ER kinase; EIF2α, eukaryotic translation initiation factor 2; siRNA, small interfering RNA; ATF6, activating transcription factor 6.

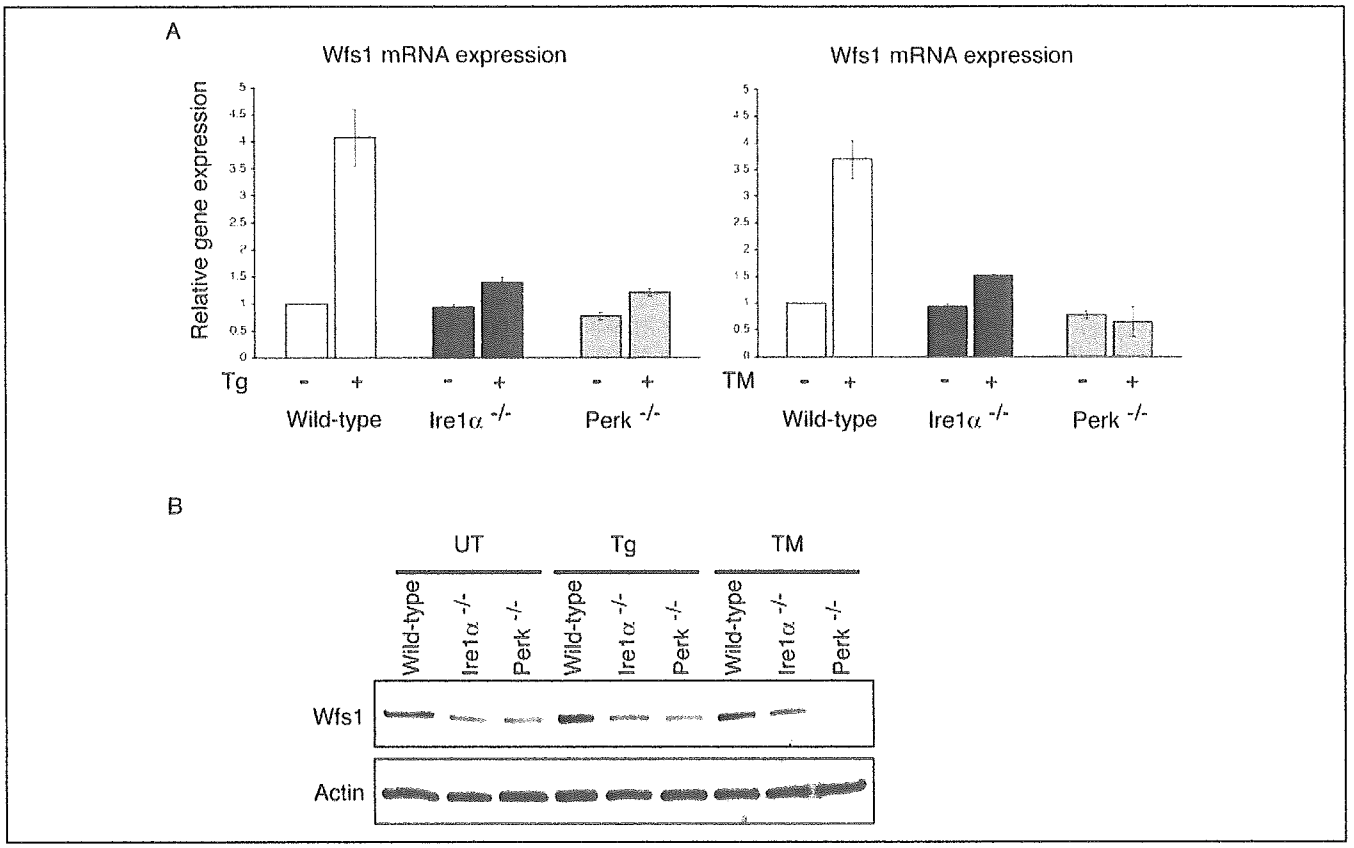

FIGURE 1. **Expression of WFS1, a component of the UPR, is regulated by Ire1α.** *A*, quantitative real time PCR of WFS1 using reverse-transcribed RNA from wild-type, Ire1α knock-out (Ire1$\alpha^{-/-}$), and Perk knock-out (Perk$^{-/-}$) mouse embryonic fibroblasts. Cells were untreated (*UT*) or treated with thapsigargin (*Tg*) or tunicamycin (*TM*) for 3 h. The amount of mouse WFS1 mRNA was normalized to the amount of actin mRNA in each sample (n = 3; values are mean ± S.E.). *B*, immunoblot analysis of WFS1 protein using lysates from wild-type, Ire1α knock-out (Ire1$\alpha^{-/-}$), and Perk knock-out (Perk$^{-/-}$) mouse embryonic fibroblasts. Cells were untreated or treated with thapsigargin (*Tg*) or tunicamycin (*TM*) for 3 h. The amount of actin is shown in the *lower panel*.

in the *EIF2AK3* gene encoding PERK have been reported (32). PERK knock-out mice also develop diabetes because of the high level of ER stress in the pancreas (33, 34), strongly suggesting that β-cell death in patients with Wolcott-Rallison syndrome is caused by ER stress. ATF6 is a bZIP-containing transcription factor in the ER. Under ER stress, ATF6 is cleaved and released from the ER. The bZIP domain of ATF6 then translocates into the nucleus and up-regulates the UPR-specific downstream genes. The physiological role of ATF6 in pancreatic β-cells is not yet known.

Increasing evidence suggests that a high level of ER stress and defective ER stress signaling are important in the pathogenesis of diabetes. It is highly likely that downstream components of ER stress signaling maintain ER homeostasis in pancreatic β-cells. Therefore, defective ER stress signaling could cause a high level of ER stress in pancreatic β-cells and lead to β-cell dysfunction and diabetes. Pancreatic β-cells are specialized in proinsulin folding and insulin secretion. It is possible that β-cells have a unique downstream component of ER stress signaling. In this study we investigated whether Wolfram syndrome gene 1 (*WFS1*) is a component of ER stress signaling and has a function in maintaining ER homeostasis in β-cells.

EXPERIMENTAL PROCEDURES

Plasmids, Cell Culture, and Transfection—INS-1 832/13 cells were a gift from Dr. Christopher Newgard (Duke University Medical Center). INS-1 832/13 cells were maintained in RPMI with 10% fetal bovine serum and transfected with siRNA for WFS1 using the Cell Line Nucleofector™ T kit and the Nucleofector device (Amaxa Biosystems, Gaithersburg, MD). siRNAs were designed and synthesized at Qiagen (Valencia, CA) as follows: for rat WFS1–1, AAGGCATGAAGGTCTACAATT; for rat WFS1–2, AAGGCCATCAGCTGCCTCAAT. COS7 cells were maintained in Dulbecco's modified Eagle's medium with 10% fetal bovine serum and then transfected with WFS1 expression vectors using FuGENE (Roche Applied Science). Full-length human *WFS1* cDNA, as well as P724L and G695V mutant *WFS1* cDNA, were tagged with a FLAG epitope and subcloned to a pcDNA3 plasmid under the control of the cytomegalovirus promoter. The P724L and G695V mutations were introduced using the GeneTailor site-directed mutagenesis system (Invitrogen). Mouse embryonic fibroblasts were maintained in Dulbecco's modified Eagle's medium with 10% fetal bovine serum. Human fibroblasts of a patient with Wolfram syndrome and a control individual were obtained, respectively, from Coriell Institute (Camden, NJ) and from Dr. Alan Permutt (Washington University School of Medicine). Human fibroblasts were maintained in Eagle's modified essential medium with 10% fetal bovine serum.

Immunostaining—COS7 cells and frozen sections of mouse pancreata were fixed in 2% paraformaldehyde for 30 min at room temperature and then permeabilized with 0.1% Triton X-100 for 2 min. The fixed cells were washed with phosphate-buffered saline, blocked with 10% bovine serum albumin for 30 min, and incubated in primary antibody overnight at 4 °C. The cells were washed three times in phosphate-buffered saline/Tween 0.1% and incubated with secondary antibody for 1 h at room temperature. Images were obtained with a Leica TCS SP2 AOBS confocal microscope with LCS software. FLAG M2 antibody was

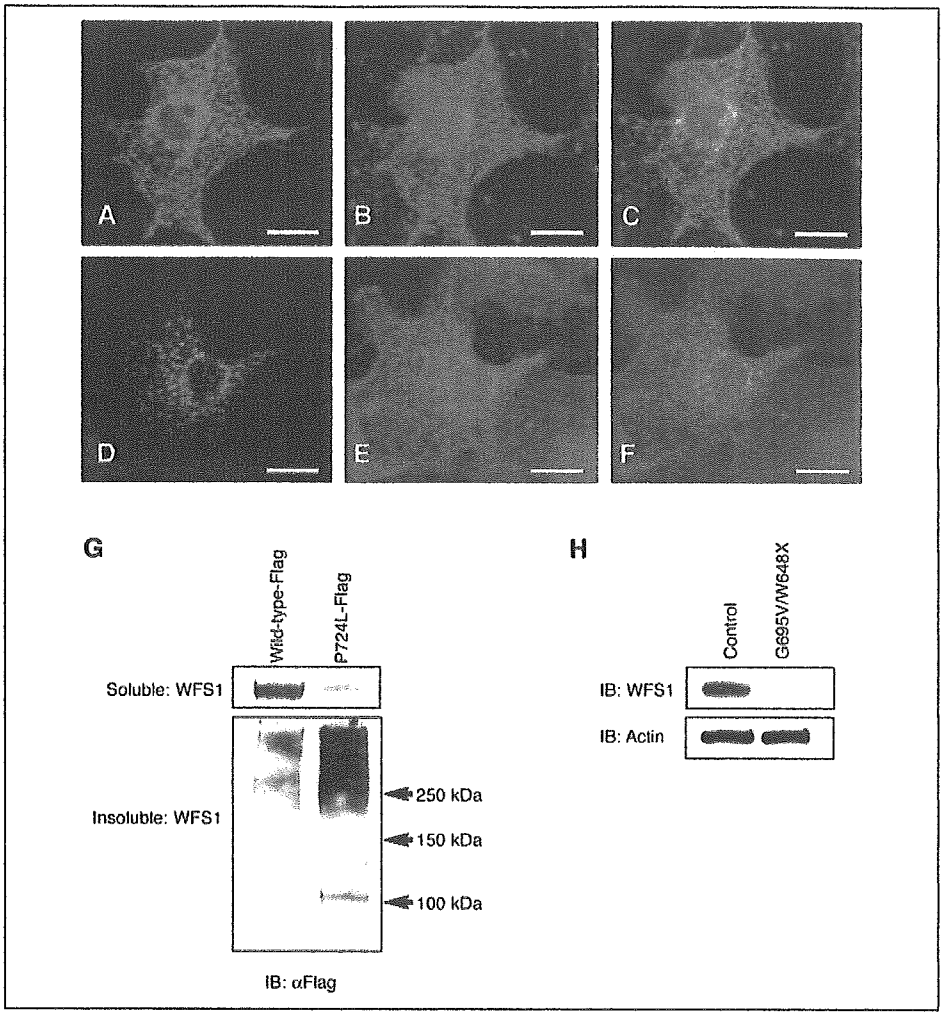

FIGURE 2. **Loss of function of WFS1 on ER membrane causes Wolfram syndrome.** Immunocytochemical staining of COS7 cells expressing FLAG-tagged human wild-type (*A–C*) or P724L WFS1 (*D–F*). Staining with anti-FLAG monoclonal antibody shows the distribution of wild-type or P724L WFS1 protein (*A* and *D*). Staining of the same cells with anti-ribophorin I antibody shows the structure of the ER (*B* and *E*). Merged images show the co-localization of WFS1 and ribophorin I (*C* and *F*). *Bars*, 10 μm. *G*, high molecular weight complexes of $WFS1^{P724L}$ in detergent-insoluble fractions. COS7 cells were transfected with FLAG-tagged wild-type or P724L WFS1 expression vector and separated into detergent-soluble (*upper panel*) and detergent-insoluble (*lower panel*) fractions and immunoblotted (*IB*) with anti-FLAG antibody. *H*, immunoblot analysis of WFS1 protein using lysates from fibroblasts of a control individual (*control*) and a patient with Wolfram syndrome carrying G695V/W648*X* mutations (G695V/W648*X*).

purchased from Sigma. Anti-WFS1 antibody was generated as described previously (35).

Immunoblotting—Fibroblasts and INS-1 832/13 cells were lysed with M-PER (Pierce) containing protease inhibitors. COS7 cells were lysed for 15 min in ice-cold buffer (20 mM Hepes, pH 7.5, 1% Triton X-100, 150 mM NaCl, 10% glycerol, 1 mM EDTA) containing protease inhibitors. Insoluble material was recovered by centrifugation at 13,000 × *g* for 15 min and solubilized in 10 mM Tris-HCl and 1% SDS for 10 min at room temperature. After the addition of 4 volumes of lysis buffer, samples were sonicated for 10 s. Lysates were separated and normalized for total protein (20 μg per lane) using 4–20% linear gradient SDS-PAGE (Bio-Rad) and then electroblotted. FLAG M2 antibody was purchased from Sigma. Anti-WFS1 antibody was generated as described previously (35).

Isolating Islets from Mouse Pancreas—Mice were anesthetized, and their pancreatic islets were then isolated by pancreatic duct injection of 5 ml (0.85 mg/ml) of collagenase solution followed by digestion at 37 °C for 25 min with mild shaking. Digestion was stopped by adding ice-cold RPMI with 1% horse serum. Islets were washed several times with RPMI, separated from acinar cells on a Histopaque gradient, and hand-picked using a dissecting microscope.

Real Time PCR—Total RNA was isolated from the cells by RNeasy (Qiagen, Valencia, CA). 1 μg of total RNA from cells was reverse-transcribed with oligo(dT) primer. For the thermal cycle reaction, the ABI prism 7000 sequencer detection system (Applied Biosystems, Foster City, CA) was used at 50 °C for 2 min, 95 °C for 10 min, then 40 cycles at 95 °C of 15 s each, and at 60 °C for 1 min. By using mouse actin for mouse embryonic fibroblasts, human glyceraldehyde-3-phosphate dehydrogenase for human fibroblasts, mouse actin for mouse islets, and rat actin for INS-1 832/13 cells as a control, the PCR was performed in triplicate for each sample and then repeated twice for all experiments. Cyber Green (Bio-Rad) and the following sets of primers were used for real time PCR: for mouse actin, GCAAGTGCTTCTAGGCGGAC and AAGAAAGGGTGTAAAACGCAGC; for mouse WFS1, CCATCAACATGCTCCCGTTC and GGGTAGGCCTCGCCATACA; for rat actin, GCAAATGCTTCTAGGCGGAC and AAGAAAGGGTGTAAAACGCAGC; and for rat WFS1, CATCACCAAGGACATCGTCCT and AGCACGTCCTTGAACTCGCT.

RESULTS

WFS1 Is a Component of the IRE1 Signaling Pathway—The pathogenesis of Wolfram syndrome has been attributed to mutations in the *WFS1* gene (35, 36). The *WFS1* gene encodes a 100-kDa glycoprotein containing 9–10 transmembrane domains that localizes to the ER (5, 6). Membrane proteins in the ER are often involved in the UPR (8, 37).

Measuring the expression levels of WFS1 by real time PCR, we found that WFS1 mRNA is induced by ER stress and is under the control of IRE1α and PERK. In wild-type mouse fibroblasts, induction of WFS1 mRNA was increased 3–5-fold by two ER stress inducers, tunicamycin and thapsigargin (Fig. 1*A*).

In Ire1$\alpha^{-/-}$ and Perk$^{-/-}$ cells, WFS1 induction was attenuated (Fig. 1*A*). By measuring WFS1 protein expression levels by immunoblot using anti-WFS1 antibody, we found that WFS1 protein expression was decreased in Ire1$\alpha^{-/-}$ and Perk$^{-/-}$ cells as compared with wild-type cells (Fig. 1*B*). Although there was a marked induction of WFS1 mRNA in wild-type cells by both inducers of ER stress (Fig. 1*A*), induction of WFS1 at the protein level in tunicamycin-treated cells in which *N*-glycosylation was inhibited was modest (Fig. 1*B*), suggesting that the WFS1 protein is unstable when *N*-glycosylation is inhibited. Also, there was no significant difference in WFS1 mRNA content between wild-type cells and both knock-out cells, although at the protein level, both Ire1$\alpha^{-/-}$ and Perk$^{-/-}$ cells exhibited a profound decrease in WFS1 protein expression. This suggests further that WFS1 protein becomes unstable by chronic high levels of ER stress because there exists a higher base-line ER stress level in Ire1$\alpha^{-/-}$ and Perk$^{-/-}$ cells, which are deficient in ER stress signaling. These results indicate that WFS1 is a component of the UPR and that its mRNA expression is regulated by the IRE1 and PERK signaling pathways.

Mutant WFS1 Does Not Accumulate on the ER Membrane—It has been reported that *WFS1* gene mutations lead to loss of function of WFS1 protein. Nonsense or frameshift mutations of the *WFS1* gene lead to a complete absence of WFS1 protein because of instability of the mutant protein (36). To extend this observation, we examined the cellular localization of mutant WFS1 protein. Most of the *WFS1* gene mutations in patients with Wolfram syndrome occur in exon 8, which encodes the transmembrane of the protein and in C-terminal luminal domains (5, 6). We cloned the full-length human *WFS1* gene by using human EST clones and then introduced into it the P724L and G695V mutations, which occur in Wolfram syndrome, by means of PCR-based mutagenesis. Like most *WFS1* mutations in Wolfram syndrome patients, the P724L and G695V mutations occurred in exon 8.

We then determined the cellular localization of wild-type and mutant WFS1 by immunostaining cells transfected with an expression vector for wild-type, P724L, or G695V WFS1 tagged at its C terminus with a FLAG epitope. Immunostaining of cells expressing wild-type WFS1 showed a diffuse reticular pattern that co-localized with the ER marker ribophorin I (Fig. 2, *A–C*). However, immunostaining with anti-FLAG antibody of cells expressing mutant WFS1 showed a punctate staining pattern in the ER, suggesting that WFS1 tends to aggregate there (Fig. 2, *D–F*). Part of WFS1^{P724L} showed a diffuse reticular pattern and was co-localized with ribophorin I, suggesting that this part of WFS1^{P724L} is localized to the ER membrane (Fig. 2, *D–F*). These staining patterns suggest that, in contrast to wild-type WFS1, most of the newly synthesized WFS1^{P724L} protein aggregates and thus is not expressed on the ER membrane. We obtained similar results by expressing WFS1^{G695V} (data not shown).

When we assessed the aggregation of WFS1^{P724L} by SDS-PAGE immunoblot analysis of detergent-soluble and detergent-insoluble lysates from COS7 cells transiently expressing these proteins, we found that the formation of insoluble and high molecular weight complexes was much more prominent in cells expressing WFS1^{P724L} than in cells expressing wild-type WFS1 (Fig. 2*G*, *lower panel*).

We also measured WFS1 protein expression levels in fibroblasts from a patient with Wolfram syndrome and a control individual. We found that WFS1 protein could not be detected in the patient sample (Fig. 2*H*), suggesting that mutant WFS1 protein in patients with Wolfram syndrome does not accumulate in cells or can no longer be detected by the antibody because of a conformational change. Our results indicate that most of the newly synthesized mutant WFS1 protein tends to aggregate and does not fold into a proper three-dimensional structure. Therefore, it is likely that Wolfram syndrome is caused by a loss of function of WFS1.

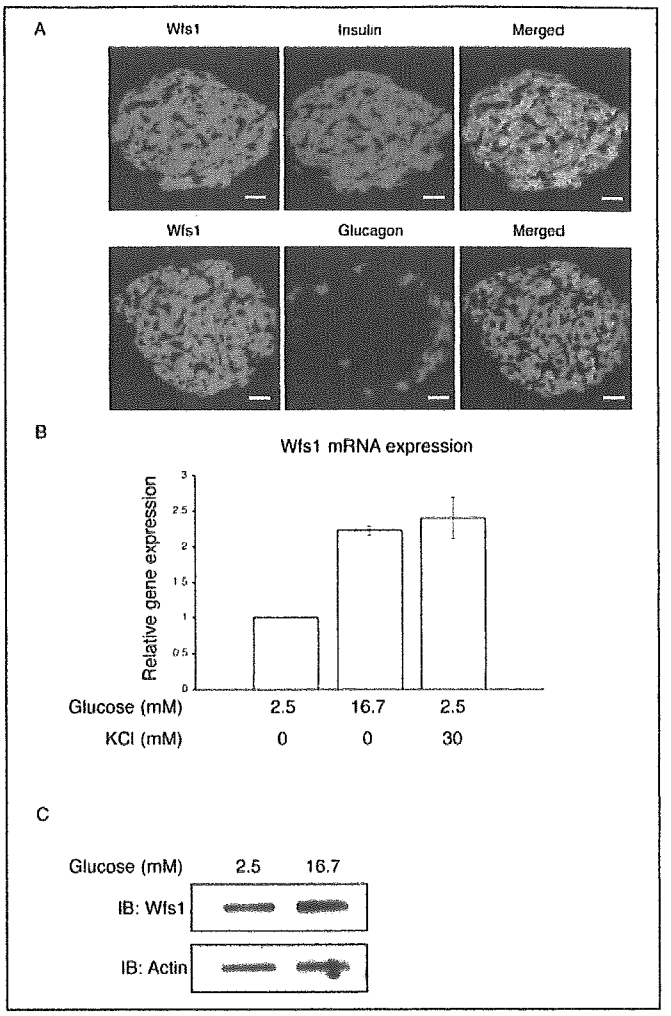

FIGURE 3. **WFS1 maintains ER homeostasis in pancreatic β-cells.** *A*, distribution of WFS1 in mouse pancreata analyzed by immunohistochemistry using anti-WFS1, anti-insulin, and anti-glucagon antibodies. Merged image shows the co-localization of WFS1 and insulin (*upper panel*) or WFS1 and glucagon (*lower panel*). *Scale bars*, 50 μm. *B*, WFS1 mRNA is up-regulated by insulin secretagogues. Mouse islets were pretreated with 2.5 mM glucose for 1 h and stimulated with 16.7 mM glucose and 30 mM KCl for 1 h. Expression levels of WFS1 and actin were then measured by real time PCR ($n = 3$; values are mean ± S.E.). *C*, WFS1 protein is up-regulated by high glucose. Mouse islets were pretreated with 2.5 mM glucose for 2 h and stimulated with 16.7 mM glucose. The expression levels of WFS1 and actin were measured by immunoblot (*IB*).

WFS1 Is Important in Sustaining ER Homeostasis in Pancreatic β-Cells—In immunohistochemistry experiments on mouse pancreata using anti-WFS1, anti-insulin, and anti-glucagon antibodies, we detected WFS1 mainly in the islets, where it co-localized with insulin (Fig. 3*A*). However, WFS1 did not co-localize with glucagon, indicating that WFS1 is especially important in the function of β-cells.

It has been shown that WFS1 has an important function in stimulus-secretion coupling in insulin secretion (38). To determine *WFS1* gene expression levels during insulin secretion, we pretreated mouse islets for 1 h with 2.5 mM glucose and then stimulated these cells for insulin secretion with 16.7 mM glucose and 30 mM KCl. *WFS1* gene expression increased after treatment with both 16.7 mM glucose and 30 mM KCl but not after treatment with 2.5 mM glucose (Fig. 3*B*), suggesting that WFS1 up-regulation is important for insulin secretion. By measuring WFS1

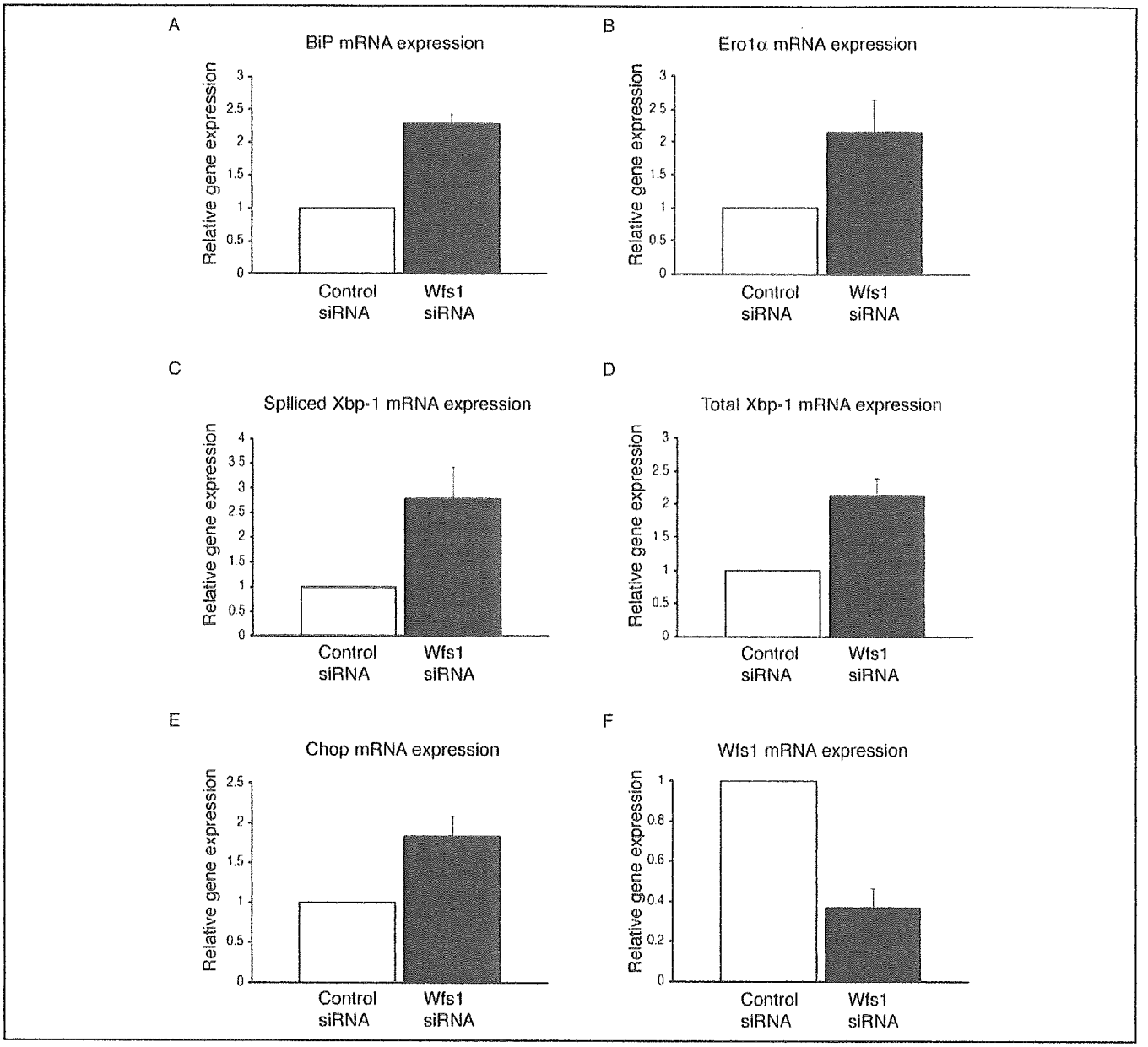

FIGURE 4. **Inhibition of WFS1 expression causes a high level of ER stress in pancreatic β-cells.** INS-1 832/13 cells were pretreated with 5 mM glucose and transfected with siRNA for WFS1 or scramble siRNA. Expression levels of the ER stress markers BiP (*A*), ERO1α (*B*), spliced XBP-1 (*C*), total XBP-1 (*D*), Chop (*E*), and WFS1 (*F*) were measured by real time PCR ($n = 3$; values are mean ± S.E.).

protein expression levels by immunoblot using anti-WFS1 antibody, we confirmed this WFS1 induction by 16.7 mM glucose in mouse islets (Fig. 3*C*).

ER homeostasis is important for insulin secretion because proinsulin, the insulin precursor, must be folded into its proper three-dimensional structure in the ER in order to become mature insulin. As a direct means of examining the relationship between the loss of function of WFS1 and ER homeostasis, we knocked down WFS1 expression in a β-cell line, INS-1 832/13, using siRNA for WFS1. The suppression of WFS1 caused an increase in the expression of BiP (Fig. 4*A*), Ero1α (Fig. 4*B*), spliced XBP-1 (Fig. 4*C*), and total XBP-1 (Fig. 4*D*), markers for ER stress in INS-1 832/13 cells. This suppression also increased the expression of another ER stress marker, Chop (Fig. 4*E*). However, the induction of Chop mRNA was modest as compared with its usual up-regulation under ER stress. Because Chop is a downstream component of Perk signaling (39), this suggests that eIF2α phosphorylation by Perk in response to WFS1 suppression is modest. Indeed, we could not detect eIF2α phosphorylation by suppressing WFS1 expression in INS-1 832/13 cells (data not shown). These results indicate that WFS1 has an important function in mitigating high levels of ER stress and in maintaining ER homeostasis in pancreatic β-cells. Therefore, suppression of WFS1 in β-cells could cause chronic ER stress in these cells.

To analyze the WFS1 expression level under pathological conditions, we measured WFS1 mRNA induction in islets from the ob/ob diabetes mouse model. We isolated islets from diabetic ob/ob mice and control C57Bl6 mice and measured WFS1 mRNA induction by treating the cells with 16.7 mM glucose. We found that induction of WFS1 mRNA was significantly more attenuated in ob/ob mice than in control mice (Fig. 5). This suggests that β-cells in ob/ob mice are in a state of chronic ER stress and that WFS1 induction is saturated.

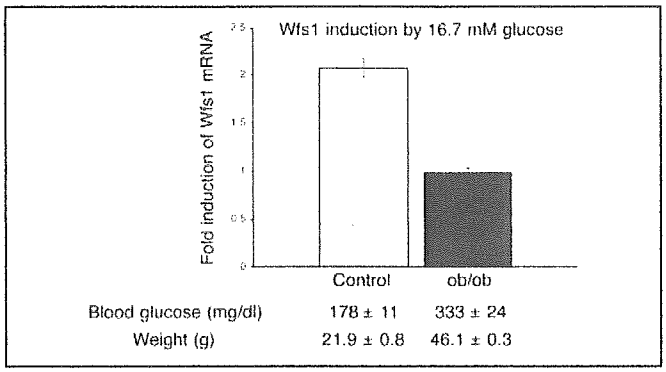

FIGURE 5. **WFS1 induction is attenuated in the islets of ob/ob mice.** Islets from control C57BL6 mice and ob/ob mice were isolated and pretreated with 2.5 mM glucose for 1 h and then stimulated with 2.5 or 16.7 mM glucose for 1 h. The expression levels of WFS1 and actin were measured by real time PCR, and the induction of WFS1 by 16.7 mM glucose was calculated ($n = 3$; values are mean ± S.E.)

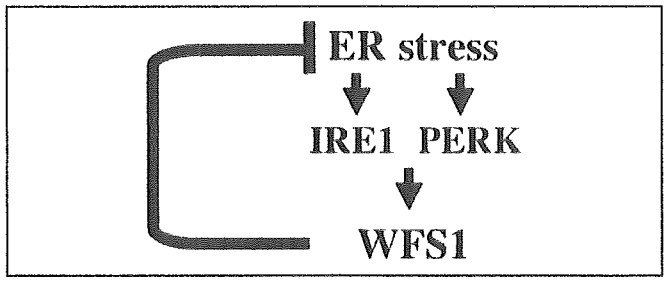

FIGURE 6. **Schematic model of the role of WFS1 in mitigating ER stress.** WFS1 is a component of IRE1 and PERK signaling (*i.e.* the UPR) and is important in the maintenance of ER homeostasis, specifically in pancreatic β-cells.

DISCUSSION

Our study has shown that WFS1 is a component of IRE1 and PERK signaling (*i.e.* the UPR) and is important in the maintenance of ER homeostasis, specifically in pancreatic β-cells (Fig. 6). *WFS1* mutations in patients with Wolfram syndrome lead to loss of function of WFS1. In addition, by using siRNA, we have shown that the suppression of WFS1 leads to a high level of ER stress in pancreatic β-cells. These findings suggest that WFS1 protects β-cells against ER stress and, conversely, that chronic ER stress is caused by loss of function of WFS1. Previous studies have shown that WFS1 protein serves as a regulator of the ER ion channel, most likely acting as a calcium channel (7, 36). It has also been reported that the increase in production of cytosolic Ca^{2+} in response to glucose is lower in the islets of WFS1 knock-out mice than it is in control mice (38). These findings suggest that loss of function of WFS1 causes abnormal calcium homeostasis in the ER and elicits ER stress, leading to the death of pancreatic β-cells.

Our findings suggest that the pathogenesis of Wolfram syndrome can be attributed to a very high level of chronic ER stress because of the lack of functional WFS1 protein in pancreatic β-cells (Fig. 4, *A–F*). WFS1 protein is expressed mainly in β-cells of the islets, but not in α-cells or exocrine acinar cells. Although α-cells and acinar cells are also active in protein secretion, WFS1 expression levels in these cells are much lower than those in β-cells that are specialized in insulin biosynthesis and secretion. Therefore, our findings of WFS1 expression only in β-cells and of WFS1 up-regulation during insulin secretion suggest that WFS1 is an important component of proinsulin folding and processing in the ER of β-cells.

Our results also show that pathogenic WFS1 mutants do not accumulate in the soluble fraction of cells and make insoluble aggregates. It is possible that the accumulation of pathogenic WFS1 mutants is toxic to pancreatic β-cells, causing them to malfunction in patients with Wolfram syndrome. Indeed, we found that transient expression of pathogenic WFS1 mutants caused ER stress in a pancreatic β-cell line, MIN6 (data not shown). However, stable expression of pathogenic WFS1 in MIN6 cells did not cause ER stress and did not change the viability of these cells.[4] These observations suggest that the expression of mutant WFS1 causes ER stress in pancreatic β-cells under specific conditions. It is also possible that ER stress response caused by transient and incomplete suppression of WFS1 with siRNA might differ from that caused by chronic and complete WFS1 deficiency. We plan to undertake additional studies to explore these possibilities.

The high levels of ER stress and pancreatic β-cell death in patients with Wolfram syndrome may be related to the β-cell dysfunction in patients with type 2 diabetes. The pathogenesis of type 2 diabetes is a result of peripheral resistance to the action of insulin, which may lead to a prolonged increase in insulin biosynthesis. Because the folding capacity of the ER is then overwhelmed, this peripheral resistance to insulin may activate the ER stress signaling pathways. For this reason, chronic ER stress in β-cells may lead to β-cell death in patients with type 2 diabetes who are genetically susceptible to ER stress. Further investigations of ER stress in the pathogenesis of diabetes are needed to obtain an understanding of the relationship between ER stress and type 2 as well as type 1B diabetes.

Acknowledgments—We thank Dr. Aldo Rossini, Dr. Rita Bortell, Dr. Shinsuke Ishigaki, Jeanne Cole, and Dr. Tomohiko Urano for comments on the manuscript. We thank Dr. Christopher Newgard for INS-1 832/13 and Dr. Alan Permutt for fibroblasts from a patient with Wolfram syndrome. We also thank Karen Sargent, Elaine Norowski, and Linda Leehy for technical assistance.

REFERENCES

1. Wolfram, D. J., and Wagener, H. P. (1938) *Mayo Clin. Proc.* **1,** 715–718
2. Barrett, T. G., and Bundey, S. E. (1997) *J. Med. Genet.* **34,** 838–841
3. Rando, T. A., Horton, J. C., and Layzer, R. B. (1992) *Neurology* **42,** 1220–1224
4. Karasik, A., O'Hara, C., Srikanta, S., Swift, M., Soeldner, J. S., Kahn, C. R., and Herskowitz, R. D. (1989) *Diabetes Care* **12,** 135–138
5. Inoue, H., Tanizawa, Y., Wasson, J., Behn, P., Kalidas, K., Bernal-Mizrachi, E., Mueckler, M., Marshall, H., Donis-Keller, H., Crock, P., Rogers, D., Mikuni, M., Kumashiro, H., Higashi, K., Sobue, G., Oka, Y., and Permutt, M. A. (1998) *Nat. Genet.* **20,** 143–148
6. Strom, T. M., Hortnagel, K., Hofmann, S., Gekeler, F., Scharfe, C., Rabl, W., Gerbitz, K. D., and Meitinger, T. (1998) *Hum. Mol. Genet.* **7,** 2021–2028
7. Osman, A. A., Saito, M., Makepeace, C., Permutt, M. A., Schlesinger, P., and Mueckler, M. (2003) *J. Biol. Chem.* **278,** 52755–52762
8. Harding, H. P., Calfon, M., Urano, F., Novoa, I., and Ron, D. (2002) *Annu. Rev. Cell Dev. Biol.* **18,** 575–599
9. Kaufman, R. J., Scheuner, D., Schroder, M., Shen, X., Lee, K., Liu, C. Y., and Arnold, S. M. (2002) *Nat. Rev. Mol. Cell. Biol.* **3,** 411–421
10. Mori, K. (2000) *Cell* **101,** 451–454
11. Harding, H. P., and Ron, D. (2002) *Diabetes* **51,** Suppl. 3, 455–461
12. Scheuner, D., Gromeier, M., Davies, M. V., Dorner, A. J., Song, B., Patel, R. V., Wimmer, E. J., McLendon, R. E., and Kaufman, R. J. (2003) *Virology* **317,** 263–274
13. Kaufman, R. J. (2002) *J. Clin. Investig.* **110,** 1389–1398
14. Tirasophon, W., Welihinda, A. A., and Kaufman, R. J. (1998) *Genes Dev.* **12,** 1812–1824
15. Iwawaki, T., Akai, R., Kohno, K., and Miura, M. (2004) *Nat. Med.* **10,** 98–102
16. Wang, X. Z., Harding, H. P., Zhang, Y., Jolicoeur, E. M., Kuroda, M., and Ron, D. (1998) *EMBO J.* **17,** 5708–5717
17. Bertolotti, A., Wang, X., Novoa, I., Jungreis, R., Schlessinger, K., Cho, J. H., West, A. B., and Ron, D. (2001) *J. Clin. Investig.* **107,** 585–593
18. Calfon, M., Zeng, H., Urano, F., Till, J. H., Hubbard, S. R., Harding, H. P., Clark, S. G., and Ron, D. (2002) *Nature* **415,** 92–96
19. Yoshida, H., Matsui, T., Hosokawa, N., Kaufman, R. J., Nagata, K., and Mori, K. (2003) *Dev. Cell* **4,** 265–271
20. Urano, F., Wang, X., Bertolotti, A., Zhang, Y., Chung, P., Harding, H. P., and Ron, D.

[4] S. G. Fonseca, M. Fukuma, K. L. Lipson, L. X. Nguyen, J. R. Allen, Y. Oka, and F. Urano, unpublished observations.

(2000) *Science* **287,** 664–666
21. Hoeflich, K. P., Yeh, W. C., Yao, Z., Mak, T. W., and Woodgett, J. R. (1999) *Oncogene* **18,** 5814–5820
22. Nishitoh, H., Saitoh, M., Mochida, Y., Takeda, K., Nakano, H., Rothe, M., Miyazono, K., and Ichijo, H. (1998) *Mol. Cell* **2,** 389–395
23. Nishitoh, H., Matsuzawa, A., Tobiume, K., Saegusa, K., Takeda, K., Inoue, K., Hori, S., Kakizuka, A., and Ichijo, H. (2002) *Genes Dev.* **16,** 1345–1355
24. Ozcan, U., Cao, Q., Yilmaz, E., Lee, A. H., Iwakoshi, N. N., Ozdelen, E., Tuncman, G., Gorgun, C., Glimcher, L. H., and Hotamisligil, G. S. (2004) *Science* **306,** 457–461
25. Yoneda, T., Imaizumi, K., Oono, K., Yui, D., Gomi, F., Katayama, T., and Tohyama, M. (2001) *J. Biol. Chem.* **276,** 13935–13940
26. Nakagawa, T., Zhu, H., Morishima, N., Li, E., Xu, J., Yankner, B. A., and Yuan, J. (2000) *Nature* **403,** 98–103
27. Yoshida, H., Haze, K., Yanagi, H., Yura, T., and Mori, K. (1998) *J. Biol. Chem.* **273,** 33741–33749
28. Yoshida, H., Okada, T., Haze, K., Yanagi, H., Yura, T., Negishi, M., and Mori, K. (2000) *Mol. Cell. Biol.* **20,** 6755–6767
29. Harding, H. P., Zhang, Y., and Ron, D. (1999) *Nature* **397,** 271–274
30. Shi, Y., Vattem, K. M., Sood, R., An, J., Liang, J., Stramm, L., and Wek, R. C. (1998) *Mol. Cell. Biol.* **18,** 7499–7509
31. Harding, H. P., Zhang, Y., Bertolotti, A., Zeng, H., and Ron, D. (2000) *Mol. Cell* **5,** 897–904
32. Delepine, M., Nicolino, M., Barrett, T., Golamaully, M., Lathrop, G. M., and Julier, C. (2000) *Nat. Genet.* **25,** 406–409
33. Harding, H. P., Zeng, H., Zhang, Y., Jungries, R., Chung, P., Plesken, H., Sabatini, D. D., and Ron, D. (2001) *Mol. Cell* **7,** 1153–1163
34. Zhang, P., McGrath, B., Li, S., Frank, A., Zambito, F., Reinert, J., Gannon, M., Ma, K., McNaughton, K., and Cavener, D. R. (2002) *Mol. Cell. Biol.* **22,** 3864–3874
35. Takeda, K., Inoue, H., Tanizawa, Y., Matsuzaki, Y., Oba, J., Watanabe, Y., Shinoda, K., and Oka, Y. (2001) *Hum. Mol. Genet.* **10,** 477–484
36. Hofmann, S., Philbrook, C., Gerbitz, K. D., and Bauer, M. F. (2003) *Hum. Mol. Genet.* **12,** 2003–2012
37. Patil, C., and Walter, P. (2001) *Curr. Opin. Cell Biol.* **13,** 349–355
38. Ishihara, H., Takeda, S., Tamura, A., Takahashi, R., Yamaguchi, S., Takei, D., Yamada, T., Inoue, H., Soga, H., Katagiri, H., Tanizawa, Y., and Oka, Y. (2004) *Hum. Mol. Genet.* **13,** 1159–1170
39. Harding, H. P., Novoa, I., Zhang, Y., Zeng, H., Wek, R., Schapira, M., and Ron, D. (2000) *Mol. Cell* **6,** 1099–1108

Diabetologia (2005) 48: 984–992
DOI 10.1007/s00125-005-1735-1

ARTICLE

N. Shojima · T. Ogihara · K. Inukai · M. Fujishiro · H. Sakoda · A. Kushiyama · H. Katagiri · M. Anai · H. Ono · Y. Fukushima · N. Horike · A. Y. I. Viana · Y. Uchijima · H. Kurihara · T. Asano

Serum concentrations of resistin-like molecules β and γ are elevated in high-fat-fed and obese *db/db* mice, with increased production in the intestinal tract and bone marrow

Received: 2 June 2004 / Accepted: 3 December 2004 / Published online: 15 April 2005

Abstract *Aims/hypothesis:* Resistin and the resistin-like molecules (RELMs) comprise a novel class of cysteine-rich proteins. Among the RELMs, RELMβ and RELMγ are produced in non-adipocyte tissues, but the regulation of their expression and their physiological roles are largely unknown. We investigated in mice the tissue distribution and dimer formation of RELMβ and RELMγ and then examined whether their serum concentrations and tissue expression levels are related to insulin resistance. *Methods:* Specific antibodies against RELMβ and RELMγ were generated. Dimer formation was examined using COS cells and the colon. RELMβ and RELMγ tissue localisation and expression levels were analysed by an RNase protection assay, immunoblotting and immunohistochemical study. Serum concentrations in high-fat-fed and *db/db* mice were also measured using the specific antibodies. *Results:* The intestinal tract produces RELMβ and RELMγ, and colonic epithelial cells in particular express both RELMβ and RELMγ. In addition, RELMβ and RELMγ were shown to form a homodimer and a heterodimer with each other, in an overexpression system using cultured cells, and in mouse colon and serum. Serum RELMβ and RELMγ levels in high-fat-fed mice were markedly higher than those in mice fed normal chow. Serum RELMβ and RELMγ concentrations were also clearly higher in *db/db* mice than in lean littermates. Tissue expression levels revealed that elevated serum concentrations of RELMβ and RELMγ are attributable to increased production in the colon and bone marrow. *Conclusions/interpretation:* RELMβ and RELMγ form homo/heterodimers, which are secreted into the circulation. Serum concentrations of RELMβ and RELMγ may be a novel intestinal-tract-mediating regulator of insulin sensitivity, possibly involved in insulin resistance induced by obesity and a high-fat diet.

Keywords Bone marrow · *db/db* mice · Heterodimer · High-fat diet · Homodimer · Insulin resistance · Intestinal · Resistin-like molecule β · Resistin-like molecule γ · Serum concentration

Abbreviations FIZZ: found in inflammatory zone · GST: glutathione S-transferase · PPARγ: peroxisome proliferator-activated receptor γ · RELM: resistin-like molecules · XCP: ten-cysteine protein

N. Shojima · M. Fujishiro · H. Sakoda · A. Kushiyama · Y. Fukushima
Department of Internal Medicine,
Graduate School of Medicine,
University of Tokyo,
Tokyo, Japan

T. Ogihara · H. Katagiri
Division of Advanced Therapeutics for Metabolic Diseases,
Centre for Translational and Advanced Animal Research on Human Diseases, Tohoku University
Graduate School of Medicine,
Sendai, Japan

K. Inukai
The Fourth Department of Internal Medicine,
Saitama Medical School,
Iruma-gun, Saitama, Japan

M. Anai · H. Ono
The Institute for Adult Disease,
Asahi Life Foundation,
Tokyo, Japan

N. Horike · A. Y. I. Viana · Y. Uchijima · H. Kurihara · T. Asano (✉)
Department of Physiological Chemistry and Metabolism,
Graduate School of Medicine, University of Tokyo,
7-3-1 Hongo, Bunkyo-ku,
Tokyo, Japan
e-mail: asano-tky@umin.ac.jp
Tel.: +81-3-38155411
Fax: +81-3-58031874

Introduction

Type 2 diabetes is characterised by insulin resistance of peripheral tissues such as the liver and muscle and adipose tissue [1–4]. Recent studies have indicated that adipose

tissue is, in addition to being a lipid storage site, an endocrine organ producing hormones, cytokines and other substances [5–7]. Recently, resistin was newly identified as an adipocyte-secreted protein [8]. Serum resistin levels are reportedly elevated in genetically obese mice and are downregulated by administration of thiazolidinediones [9, 10], peroxisome proliferator-activated receptor γ (PPARγ) agonists, although contradictory data also exist [11]. Resistin has been demonstrated to antagonise insulin action in cultured cells such as 3T3-L1 adipocytes, as well as in rodents [8]. Resistin knock-out mice exhibited lower blood glucose with reduced hepatic glucose production [12]. Thus resistin could be one of the important adipokines causing insulin resistance.

The presence of resistin-like molecules (RELMs) indicates that resistin belongs to a novel family of cysteine-rich secreted proteins (RELM/found in inflammatory zone [FIZZ]/ten-cysteine protein [XCP]). RELMα/FIZZ1 [13] and RELMβ/FIZZ2 [14] are homologous with resistin/FIZZ3 and expressed mainly in white adipose tissue and the colon respectively [14, 15]. The administration of RELMβ to rats resulted in acute impairment of hepatic insulin sensitivity and glucose metabolism [16], which suggested RELMβ is a link between the intestine and hepatic insulin action. Finally, *RELMγ/FIZZ4/XCP1* , a fourth member of the RELM/FIZZ/XCP family, was identified as a gene with decreased expression in rat nasal respiratory epithelium exposed to cigarette smoke [17]. RELMγ was expressed in the bone marrow, spleen, pancreas and colon, and was revealed to play a role as a cytokine in haematopoiesis [18, 19].

The consensus structure of the RELMs is composed of two domains; one half is the N-terminal, including an N-terminal signal sequence and a variable middle portion, and the other half is the C-terminal domain, which has a highly conserved C-terminal signature sequence containing a unique spacing of the cysteine residues. The N-terminal domains of RELMα, RELMβ and RELMγ are 15, 35 and 17% identical to resistin, whereas the C-terminal domains are 47, 54 and 52% identical to resistin. The C-terminus of RELMγ is highly homologous (84%) with RELMβ. Recently, the crystal structures of resistin and RELMβ were revealed to have a unique multimeric structure [20]. Each protomer is comprised of a 'head' and 'tail' segment and circulates as an assembly of hexamers and trimers, which reflect activation of resistin.

We previously identified RELMγ cDNA independently by PCR using degenerated oligonucleotide primers, and investigated its tissue distribution. Since we succeeded in preparing highly specific antibodies against RELMβ and RELMγ, we were able to detect the endogenous proteins and measure serum concentrations as well as tissue contents of RELMβ and RELMγ in the mouse. In this study, we show for the first time that RELMβ and RELMγ form not only a homodimer but also a heterodimer with each other in both tissue and serum. Interestingly, we also found that the serum concentrations of RELMβ and RELMγ are significantly elevated in high-fat-diet-induced and obese diabetic mice. These observations are probably attributable to increased production in the colon and bone marrow. Thus, this report is the first to raise the possibility of a novel intestinal-tract-mediating regulatory mechanism of insulin sensitivity, which may be involved in insulin resistance induced by obesity and a high-fat diet.

Materials and methods

cDNA cloning of a novel RELM/FIZZ isoform Two degenerate oligonucleotide primers were synthesised for PCR. These primers were 5′-ATGAAGA/CCTACAA/CC/TT/GTGTTC/TC-3′ and 5′-TTAG/AGA/CCAG/TTT/CGGC GCAGCG-3′, corresponding to amino acid residues 1–8 and 104–111 of RELMα/β, which are highly conserved among RELM/FIZZ isoforms. PCR was performed using mouse embryonic cDNA. A DNA fragment of approximately 330 bp was then separated by electrophoresis, cloned into TA vector pCRII (Invitrogen, San Diego, CA, USA), and sequenced using a DNA sequencer. We obtained two independent sequences: one, F1, turned out to be completely homologous to mouse RELMα/FIZZ1; the other, F2, encoded a protein to mouse RELMγ/FIZZ4. Then, a mouse embryonic cDNA library produced by a standard method (Stratagene, La Jolla, CA, USA) was screened under standard hybridisation conditions using a ^{32}P-labelled F2 cDNA fragment as a probe to obtain a full-length cDNA encoding RELMγ/FIZZ4. Positive clones were excised into pBluescript and sequenced.

RNase protection assay of various tissues Mice were killed by cervical dislocation, and various tissues (cerebrum, cerebellum, brainstem, heart, lung, liver, oesophagus, stomach, jejunum, ileum, colon, kidney, testis, spleen, pancreas, abdominal fat, epididymal fat, muscle, aorta, femoral bone marrow) were removed. Total RNA was isolated with Isogen (Nippon Gene, Japan). [α-^{32}P]UTP-labelled RNA probes were prepared using nucleotides 1–200 of mouse RELMβ, and 83–315 of mouse RELMγ as templates. An RNase protection assay was performed using an RPA III kit (Ambion, Austin, TX, USA) according to the manufacturer's instructions.

Preparation of the antibodies An antibody against the whole mouse resistin molecule was prepared by immunising rabbits with the recombinant mouse resistin protein, obtained as described previously [21]. Sequences corresponding to nucleotides 11–173 of RELMβ/FIZZ2 and 47–227 of RELMγ/FIZZ4 were amplified by PCR and cloned into the pGEX-3T expression vector (Pharmacia, Piscataway, NJ, USA). Glutathione *S*-transferase (GST) fusion proteins (GST-RELMβ and GST-RELMγ) were prepared according to the manufacturer's instructions (Pharmacia). The antisera were raised by immunising rabbits with GST-RELMβ and GST-RELMγ. From these antisera, an antibody against GST protein was removed by filtering through Affigel-10 covalently coupled to GST proteins. Then, specific antibodies against RELMβ and RELMγ were affinity purified with Affigel-10 covalently

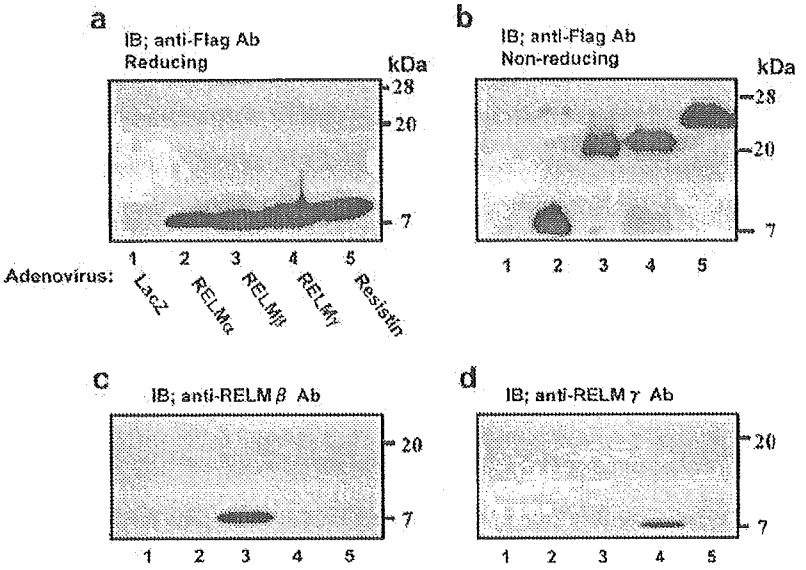

Fig. 1 Immunoblotting of RELMs secreted by COS7 cells. The four cDNAs coding RELMα, RELMβ, RELMγ and resistin, with the Flag tag at their C-termini, were expressed into COS7 cells and the medium from each cell type was subjected to SDS-PAGE under reducing (**a**, **c** and **d**) and non-reducing (**b**) conditions and immunoblotted (IB) with anti-Flag (**a**, **b**), anti-RELMβ (**c**) and anti-RELMγ (**d**) antibody (Ab)

coupled to GST-RELMβ and GST-RELMγ respectively. Antibodies against Flag tag were purchased from Upstate Biotech, Inc. (Lake Placid, NY, USA).

Immunohistochemistry Intestinal tissues removed from the mice were fixed in 10% phosphate-buffered formalin (pH 7.4) and embedded in paraffin. After sectioning, the tissues were dewaxed in ethanol, rehydrated in 10 mmol/l citric acid buffer, and microwaved for 13 min. The tissue sections were blocked with serial incubation in 30% H_2O_2, avidin D-blocking reagent, biotin-blocking reagent and protein-blocking reagent. The sections were then incubated with an affinity-purified polyclonal antibody for murine RELMβ and RELMγ or control serum at a 1:100 dilution overnight at 4°C. After washing with PBS, the slides were incubated with a biotinylated goat anti-rabbit secondary antibody followed by detection of horseradish peroxidase.

Animal studies Nine-week-old male mice (C57BL/6J) were purchased from Jackson Laboratories (Bar Harbor, ME, USA). They were divided into two groups. One group (n=9) was maintained on standard rodent chow, the other (n=9) was fed a high-fat diet (60% fat, 25% carbohydrate and 15% protein). Genetically obese *db/db* mice (n=6) and lean littermates (n=6) were purchased from Jackson Laboratories. They were maintained on standard rodent chow. Tissues from the mice were homogenised in ice-cold lysis buffer. Insoluble materials were removed and the cell lysates were incubated for 2 h at 4°C with the indicated antibody. Blood samples were centrifuged at 3,000 rev/min for 20 min and sera containing equal amounts of protein were used for immunoprecipitation. Immunoblotting against these immunoprecipitates was performed as previously described [21]. Animal care and procedures of the experiments were approved by the Animal Care Committee of the University of Tokyo.

Statistical analysis Data are expressed as means±SE. Comparisons were made using unpaired t-tests. Serum RELM levels were compared with body weight, serum glucose and insulin levels by Pearson's correlation. Values of $p<0.05$ were considered significant.

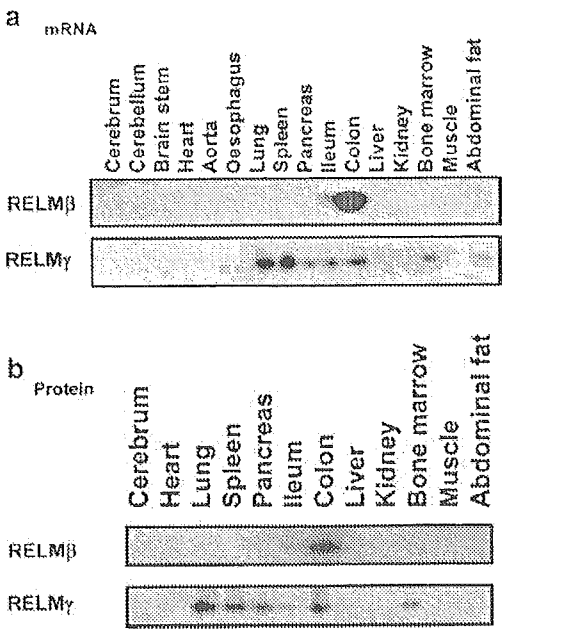

Fig. 2 RELMβ and RELMγ expression in various tissues. **a** 10 μg of RNA from various mouse tissues were prepared and hybridised with [α-^{32}P]UTP-labelled RNA probes for RELMβ or RELMγ. The RNase protection assay was performed using an RPA III kit (Ambion) according to the manufacturer's instructions. **b** Cell lysates from various mouse tissues were prepared and then immunoprecipitated and immunoblotted with anti-RELMβ antibody. Cell lysates from tissues were prepared and then immunoprecipitated and immunoblotted with anti-RELMγ antibody

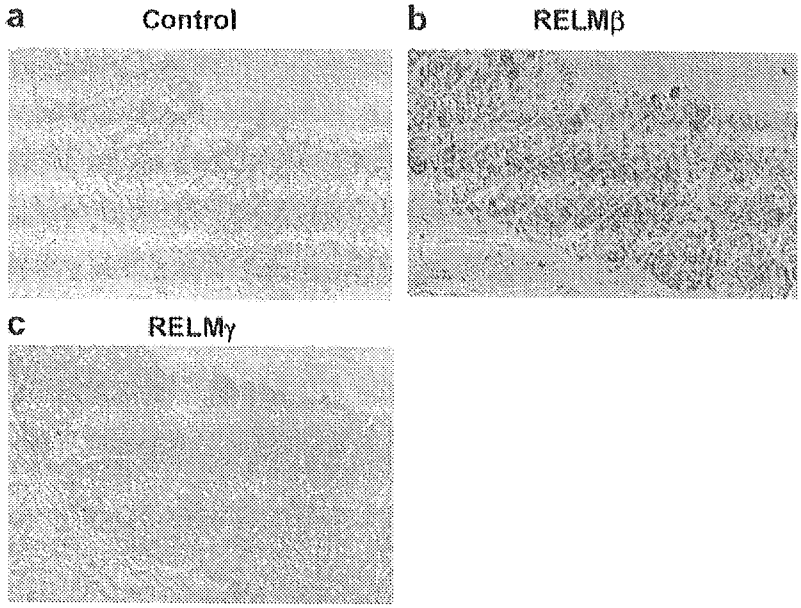

Fig. 3 Immunohistochemical study of RELMβ and RELMγ. Immunohistochemical study of the colon with control antibody (**a**) confirmed the specificities of specific antibodies (×200). The avidin–biotin–peroxidase complex method with antibodies against RELMβ (**b**) and RELMγ (**c**) was used to detect cells expressing these RELMs. RELMβ and RELMγ staining is *brown*, that of the control *blue*

Results

Cloning of RELMγ cDNA To obtain a cDNA fragment corresponding to a novel isoform of RELM/FIZZ, PCR was performed using degenerate oligonucleotides as primers and mouse embryonic cDNA as a substrate. PCR products, with a length of approximately 300–350 bp, were separated, subcloned and sequenced. Isolated PCR products were shown to consist of two different cDNAs. One corresponded to RELMα cDNA [14], the other to RELMγ. The full-length cDNAs encoding resistin, RELMα and RELMβ were prepared by PCRs based on the reported sequences. The full-length cDNA encoding RELMγ was obtained by screening a cDNA library.

Overexpression of RELMs in COS7 cells and preparation of specific antibodies against RELMβ and RELMγ Four cDNAs encoding RELMα, RELMβ, RELMγ and resistin, with the Flag tag at their C-termini, were ligated into adenovirus expression vectors. COS7 cells were infected with these adenoviruses to achieve similar protein expression levels, as assessed by immunoblotting using anti-Flag antibody. The media from cells transfected with these adenoviruses were subjected to SDS-PAGE and immunoblotted with anti-Flag antibody (Fig. 1a). The expression of these proteins was observed as very similar band densities of 7–12 kDa. Thus, it was clear that RELMγ was secreted into the media, like other members of the RELM family, when expressed in COS7 cells.

Next, we investigated the electrophoretic mobilities of these RELMs under non-reducing conditions. As shown in Fig. 1b, RELMβ, RELMγ and resistin migrated with apparent molecular masses twice those of the respective monomers, whereas RELMα behaved as a monomer. Taking previous [22, 23] and current results into account, it was confirmed that resistin, RELMβ and RELMγ form a

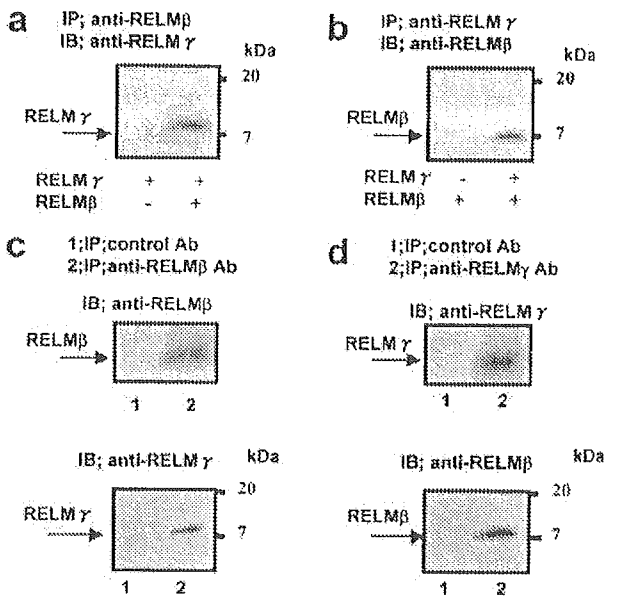

Fig. 4 Heterodimer formations of RELMβ/RELMγ (**a**, **b**) in COS7 cells and endogenous RELMβ/RELMγ in colon (**c**, **d**). **a** Secreted RELMγ, co-expressed with (*right lane*) or without (*left lane*) RELMβ, was immunoprecipitated (*IP*) with anti-RELMβ antibody (*Ab*) and then immunoblotted with anti-RELMγ Ab. **b** RELMβ, co-expressed with (*right lane*) or without (*left lane*) RELMγ was immunoprecipitated with anti-RELMγ Ab and immunoblotted with anti-RELMβ Ab. **c** Colon cell lysates were immunoprecipitated with control IgG (*lane 1*) and anti-RELMβ Ab (*lane 2*) and then immunoblotted with anti-RELMβ Ab (*upper panel*) and anti-RELMγ Ab (*lower panel*). **d** The colon cell lysates were immunoprecipitated with control IgG (*lane 1*) and anti-RELMγ Ab (*lane 2*) and immunoblotted with anti-RELMγ Ab (*upper panel*) or anti-RELMβ Ab (*lower panel*)

Table 1 Serum RELMβ and RELMγ in high-fat-fed mice

	4 weeks		8 weeks		12 weeks	
	Control	High-fat	Control	High-fat	Control	High-fat
RELMβ	1±0.05	1.08±0.06	1±0.05	1.74±0.08[a]	1±0.06	2.16±0.09[a]
RELMγ	1±0.05	1.05±0.05	1±0.06	2.00±0.10[a]	1±0.05	2.70±0.12[a]
RELMβ/γ	1±0.05	0.97±0.06	1±0.05	1.65±0.09[a]	1±0.05	2.54±0.11[a]
Body weight (g)	18.3±1.18	19.3±1.29	26.6±1.32	38.8±2.09[a]	30.1±2.07	44.4±1.95[a]
Glucose (mmol/l)	5.03±0.10	5.11±0.20	5.24±0.16	6.77±0.30	5.13±0.08	7.93±0.27[a]
Insulin (pmol/l)	22.4±1.67	22.7±2.64	26.0±5.00	48.7±2.7[a]	33.1±1.67	62.9±2.45[a]

Male 12-week-old C57BL/6J mice were fed normal chow (n=9) or a high-fat diet (n=9) from 4 to 12 weeks of age. Sera were immunoprecipitated and then immunoblotted with RELMβ and RELMγ antibody. The data are shown as ratios to the control diet values and expressed as means±SE

[a] $p<0.01$ relative to control-diet-fed mice

disulphide-linked dimer, while RELMα exists mainly as a monomer.

Immunoblotting with anti-RELMβ and anti-RELMγ antibodies (Fig. 1c, d) revealed that these antibodies do not recognise other members of the RELM/FIZZ family, suggesting anti-RELMβ and anti-RELMγ antibodies to be highly specific for the corresponding isoforms.

Tissue distribution of RELMβ and RELMγ We next evaluated RELM mRNA expression with an RNase protection assay (Fig. 2a) and protein expression using Western blotting (Fig. 2b) in various mouse tissues. RELMβ mRNA and protein were abundant in the colon, and to a lesser extent in the ileum. On the other hand, RELMγ mRNA was abundant in the colon, ileum, bone marrow, spleen, pancreas and fat, consistent with previous reports [18–20] (Fig. 2a, lower panel). RELMγ protein expression is also detectable in the colon, ileum, bone marrow, spleen and pancreas (Fig. 2b, lower panel). Thus, we found that the colon and ileum express both RELMβ and RELMγ, and the localisations of RELMβ and RELMγ were investigated by immunohistochemical staining of the colon (Fig. 3). It was demonstrated that epithelial cells throughout the crypt and surface of the colon express both RELMβ and RELMγ, while no significant staining was observed with the control antibody. The highest level of RELMβ expression was observed in goblet cells of the colon, consistent with previous reports [15, 24], and RELMγ protein

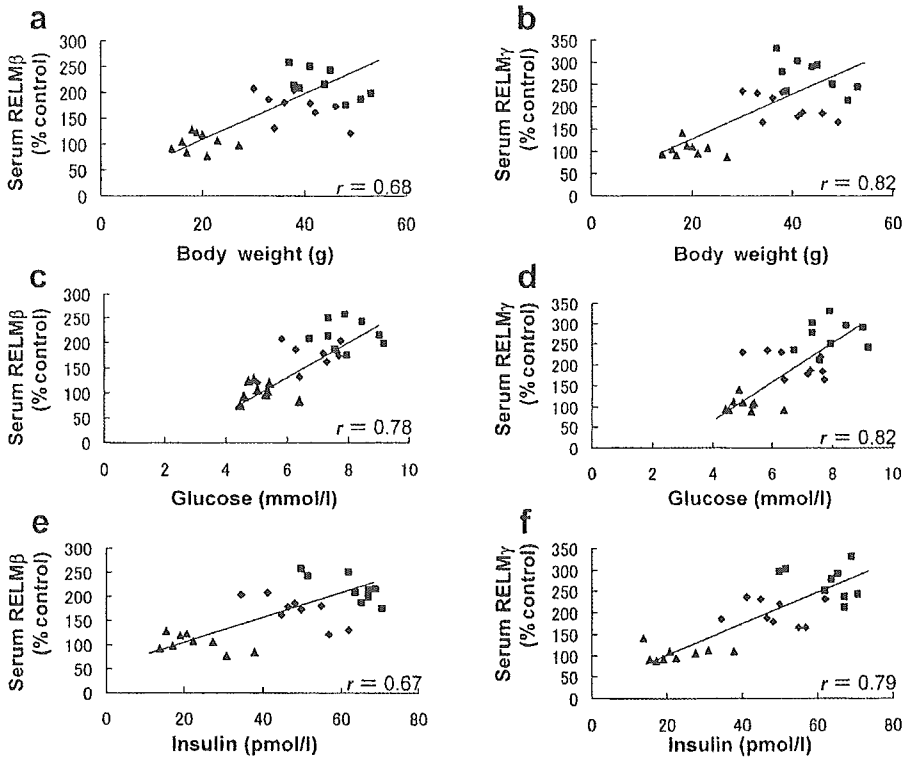

Fig. 5 Relationships between serum RELMβ and RELMγ concentration and body weight, glucose and insulin in high-fat-fed mice. Male 12-week-old C57BL/6J mice were fed normal chow (n=9) or a high-fat diet (n=9) from 4 to 12 weeks of age. RELMβ, RELMγ and various parameters were measured at 4, 8 and 12 weeks of age. The data are plotted as the percentage of the means of RELMβ and RELMγ correlated positively with body weight (**a**, $p<0.0001$; **b**, $p<0.0005$), glucose (**c**, $p<0.0005$; **d**, $p<0.0005$) and insulin (**e**, $p<0.001$; **f**, $p<0.0005$)

Table 2 Expression and regulation of mRNA and protein of RELMβ and RELMγ in high-fat-fed mice

		Colon		Bone marrow		Spleen		Lung		Pancreas	
		Control	High-fat	Control	High-fat	Control	High-fat	Control	High-fat	Control	High-fat
RELMβ	mRNA	1±0.04	1.97±0.04[a]	–	–	–	–	–	–	–	–
	Protein	1±0.03	1.96±0.05[a]	–	–	–	–	–	–	–	–
RELMγ	mRNA	1±0.04	1.84±0.03[a]	1±0.04	1.89±0.05[a]	1±0.04	1.03±0.05	1±0.04	1.05±0.05	1±0.04	0.97±0.05
	Protein	1±0.04	2.04±0.03[a]	1±0.04	1.78±0.05[a]	1±0.03	1.02±0.04	1±0.04	1.03±0.04	1±0.04	0.98±0.05

Male 12-week-old C57BL/6J mice were fed normal chow or a high-fat diet from 4 to 12 weeks of age. RNase protection assay and immunoblotting show RELMβ and RELMγ expression in the colon, bone marrow, spleen, lung and pancreas. The data are shown as ratios to the control diet values and expressed as means±SE

[a] $p<0.01$ relative to control-diet-fed mice

was also shown to be localised in goblet cells. In the bone marrow, about 30% of haematopoietic cells were stained with the anti-RELMγ antibody and these cells were myelocytes and metamyelocytes or neutrophils (data not shown), consistent with previous reports [19, 20].

Heterodimer formation between RELMβ and RELMγ in COS7 cells and tissues Since colonic cells express both RELMβ and RELMγ, we subsequently investigated whether these RELMs form a heterodimer. The RELMβ and RELMγ antibodies were highly specific and did not immunoprecipitate the respective isoforms of RELM (data not shown). As shown in Fig. 4a, b, when RELMβ and RELMγ were co-expressed, RELMγ or RELMβ was detected in the RELMβ or RELMγ immunoprecipitates respectively. These results suggest that RELMβ and RELMγ associate with each other and form a heterodimer.

Subsequently, we investigated whether or not endogenous RELMβ and RELMγ form a heterodimer using the proximal colon. RELMβ was detected in RELMγ immunoprecipitates but not in those of control antibodies (Fig. 4c). RELMγ was also detected in RELMβ immunoprecipitates but not in those of control antibodies (Fig. 4d). These results indicate that the heterodimerisation between RELMβ and RELMγ is physiological.

Increased expression of RELMβ and RELMγ in high-fat-fed mice Male 12-week-old C57BL/6J mice were fed normal chow or a high-fat diet from 4 to 12 weeks of age. A high-fat diet resulted in body weight, serum glucose and insulin increasing time-dependently (30.1±6.21 vs 44.4± 5.84 g, 5.13±0.24 vs 7.93±0.81 mmol/l, and 33.1±5.02 vs 62.9±7.35 pmol/l respectively) after 12 weeks of feeding (Table 1). Serum RELMβ and RELMγ levels were increased by 116 and 170% respectively at the end of the 12-week feeding period. We detected the RELMβ/RELMγ heterodimer in serum by immunoblotting of the anti-RELMβ immunoprecipitate with anti-RELMγ antibody, and this heterodimer was also increased.

Serum RELMβ and RELMγ and other parameters were measured at 4, 8 and 12 weeks after initiation of the high-fat diet. Close examination of these three sets of time-dependent data revealed serum RELMβ and RELMγ to correlate positively with body weight (Fig. 5a, $r=0.68$, $p< 0.0001$; Fig. 5b, $r=0.82$, $p<0.0005$), serum glucose concentration (Fig. 5c, $r=0.78$, $p<0.0005$; Fig. 5d, $r=0.82$, $p< 0.0005$) and serum insulin (Fig. 5e, $r=0.67$, $p<0.001$; Fig. 5f, $r=0.79$, $p<0.0005$).

Subsequently, we investigated the expression levels of RELMβ and RELMγ in tissues at the end of the 12-week feeding period. RELMβ mRNA and protein levels in the distal colon of the high-fat-fed mice were elevated by 97 and 96% respectively (Table 2). Similarly, RELMγ mRNA and protein levels in the distal colon were elevated by 84 and 104% respectively. RELMγ mRNA and protein levels in the bone marrow were also elevated by 89 and 78% respectively. However, no significant alterations were observed in the spleen, lung or pancreas.

Table 3 Serum RELMβ and RELMγ in *db/db* mice

	4 weeks		5 weeks		6 weeks	
	Control	*db/db*	Control	*db/db*	Control	*db/db*
RELMβ	1±0.05	1.34±0.06	1±0.06	1.57±0.09[a]	1±0.07	1.82±0.11[a]
RELMγ	1±0.06	1.68±0.04	1±0.04	1.70±0.08[a]	1±0.04	2.27±0.09[a]
RELMβ/γ	1±0.04	1.48±0.05	1±0.05	1.58±0.08[a]	1±0.05	1.79±0.06[a]
Body weight (g)	19.8±0.90	25.3±0.92	21.0±1.00	27.5±1.13	23.2±0.92	30.1±1.24[a]
Glucose (mmol/l)	4.71±0.12	5.65±0.20	4.94±0.12	5.91±0.22	4.62±0.07	6.13±0.18[a]
Insulin (pmol/l)	21.4±1.64	44.4±2.99	22.0±1.74	48.2±2.63	26.3±1.68	51.9±2.57[a]

Male lean littermates ($n=6$) and *db/db* mice ($n=6$) were fed a standard diet. Sera were immunoprecipitated and then immunoblotted with RELMβ and RELMγ antibody. The data are shown as ratios to the control lean littermate values and expressed as means±SE

[a] $p<0.01$ relative to lean littermates

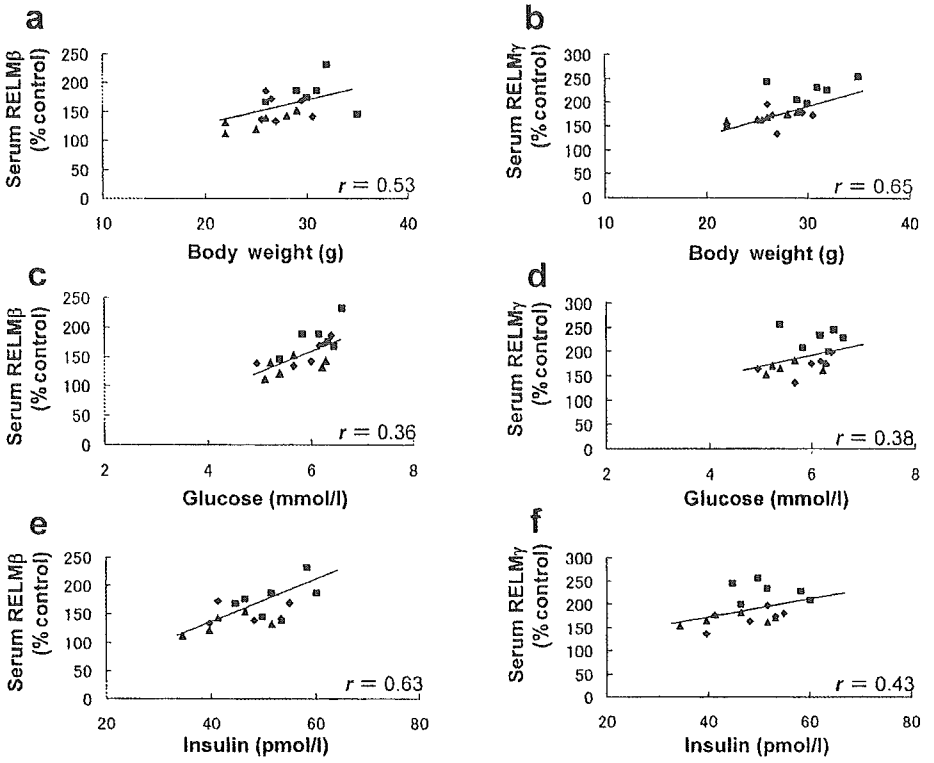

Fig. 6 Relationships between serum RELMβ and RELMγ concentrations and body weight, glucose and insulin in *db/db* mice. Male lean littermates (n=6) and *db/db* mice (n=6) were fed a standard diet. RELMβ, RELMγ and other parameters were measured at 4, 5 and 6 weeks of age. The data are plotted as percentage of the means of control lean littermates. RELMβ and RELMγ correlated positively with body weight (a, $p<0.05$; b, $p<0.01$). Neither RELMβ nor RELMγ showed any correlation with glucose (c, d). RELMβ (e, $p<0.01$), but not RELMγ (f), also positively correlated with insulin

Increased expression of RELMβ and RELMγ in db/db mice Serum RELMβ and RELMγ and other parameters in male *db/db* mice and their littermates were measured at 4, 5 and 6 weeks of age. Male 6-week-old *db/db* mice weighed more (30.1±3.03 vs 23.2±2.26 g), and had higher serum glucose (4.62±0.16 vs 6.13±0.45 mmol/l) and insulin (51.9± 6.29 vs 26.3±4.11 pmol/l), than their lean littermates. Serum RELMβ and RELMγ levels of *db/db* mice were higher and were increased by 82 and 127% respectively at the age of 6 weeks, as compared with the controls (Table 3). The RELMβ/RELMγ heterodimer in serum was also increased. Serum RELMβ and RELMγ correlated positively with body weight (Fig. 6a, r=0.53, $p<0.05$; Fig. 6b, r=0.65, $p<0.01$), but not with the serum glucose concentration (Fig. 6c, d). Serum insulin correlated positively with RELMβ (Fig. 6e, r=0.63, $p<0.01$) but not with RELMγ (Fig. 6f).

RELMβ mRNA and protein levels in the distal colons of *db/db* mice at the age of 6 weeks were elevated by 94 and 87% respectively (Table 4). Similarly, RELMγ mRNA and protein levels in the distal colon were elevated by 77 and 98% respectively (Table 4). RELMγ mRNA and protein levels in the bone marrow were elevated by 68 and 53% respectively. There were no significant changes in RELMγ levels in the spleen, lung or pancreas.

Discussion

Resistin and the three RELMs comprise a novel class of cysteine-rich proteins. Resistin is expressed exclusively in adipose tissues and reportedly causes insulin resistance [8]. RELMα was originally identified in broncho–alveolar

Table 4 Expression and regulation of mRNA and protein of RELMβ and RELMγ in *db/db* mice

		Colon		Bone marrow		Spleen		Lung		Pancreas	
		Control	*db/db*	Control	*db/db*	Control	*db/db*	Control	*db/db*	Control	*db/db*
RELMβ	mRNA	1±0.04	1.97±0.07[a]	–	–	–	–	–	–	–	–
	Protein	1±0.05	1.87±0.07[a]	–	–	–	–	–	–	–	–
RELMγ	mRNA	1±0.06	1.77±0.07[a]	1±0.07	1.63±0.07[a]	1±0.04	0.98±0.05	1±0.05	0.96±0.07	1±0.06	1.10±0.07
	Protein	1±0.05	1.98±0.07[a]	1±0.05	1.53±0.07[a]	1±0.06	1.02±0.07	1±0.05	1.05±0.07	1±0.06	1.02±0.07

Male lean littermates and *db/db* mice were fed a standard diet. RNase protection assay and immunoblotting show RELMβ and RELMγ expression in the colon, bone marrow, spleen, lung and pancreas. The data are shown as ratios to the control lean littermate values and expressed as means±SE

[a] $p<0.01$ relative to control-diet-fed mice